CHALMERS

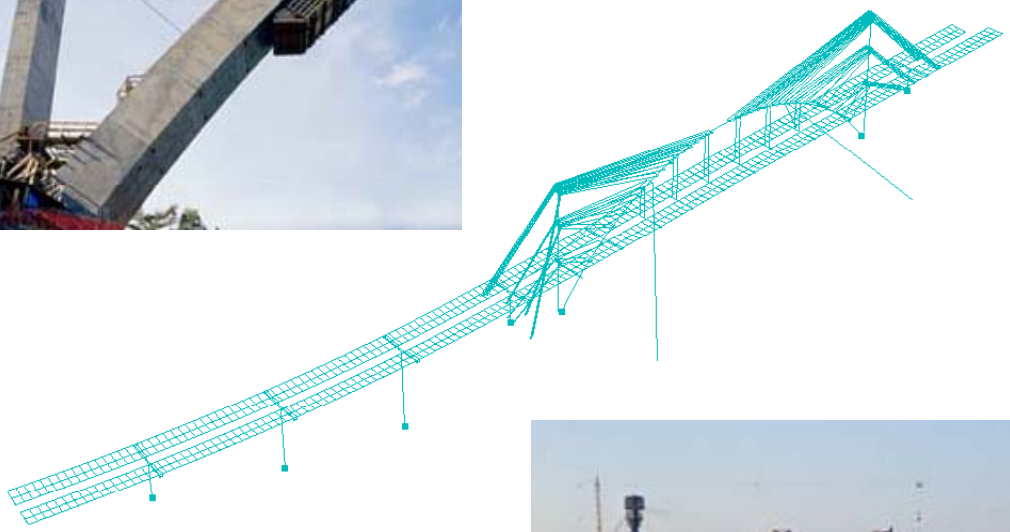

Modelling of the response of the New Svinesund Bridge

FE Analysis of the arch launching

Master's Thesis in the International Master's Programme Structural Engineering

SENAD CANOVIC AND JOAKIM GONCALVES

Department of Civil and Environmental Engineering
Division of Structural Engineering
Concrete Structures
CHALMERS UNIVERSITY OF TECHNOLOGY
Göteborg, Sweden 2005

Master's Thesis 2005:39

MASTER'S THESIS 2005:39

Modelling of the response of the New Svinesund Bridge

FE Analysis of the arch launching

Master's Thesis in the International Master's Programme Structural Engineering

SENAD CANOVIC AND JOAKIM GONCALVES

Department of Civil and Environmental Engineering
Division of Structural Engineering
Concrete Structures
CHALMERS UNIVERSITY OF TECHNOLOGY
Göteborg, Sweden 2005

Modelling the response of the New Svinesund Bridge
FE Analysis of the arch launching
Master's Thesis in the International Master's Programme Structural Engineering

SENAD CANOVIC AND JOAKIM GONCALVES

Master's Thesis 2005:39
Department of Civil and Environmental Engineering
Division of Structural Engineering
Concrete Structures
Chalmers University of Technology
SE-412 96 Göteborg
Sweden
Telephone: + 46 (0)31-772 1000

Cover:
FE model of the New Svinesund Bridge and two pictures taken during the construction of the bridge.

Chalmers reproservice
Göteborg, Sweden 2005

Modelling the response of the New Svinesund Bridge
FE Analysis of the arch launching
Master's Thesis in the International Master's Programme Structural Engineering
SENAD CANOVIC AND JOAKIM GONCALVES
Department of Civil and Environmental Engineering
Division of Structural Engineering
Concrete Structures
Chalmers University of Technology

ABSTRACT

There is a necessity to improve the methods for bridge assessment because they are over-conservative. These methods can be improved by the means of finite element (FE) analysis and field measurements. Therefore the research project "Bridge Assessment and Maintenance based on Finite Element Structural Models and Field Measurements" was initiated. The New Svinesund Bridge was chosen for practical application within this research project.

The structural model made by Bilfinger Berger during design was converted to fit the FE program ABAQUS and was further developed by introducing detailed modelling of the sequential construction of the arch. The material model for the concrete in the arch was improved in order to take into account the long-term effects of concrete, such as creep, and the development of Young's modulus with time.

The main aim was to produce a FE model that could give results in the FE analysis that are similar to the real structural behaviour of the bridge. Results considered to be of special interest were the deformations of the arch during launching, the strain variations and the sectional forces and moments within the arch. These results were compared to field measurements and other more simplified models, to evaluate the effect of different modelling.

The modelling of the sequential construction of the arch had a large influence on the sectional forces and moments. However, the modelling of viscoelastic material properties and the development of Young's modulus in concrete did not affect these results drastically. The deformations obtained during launching of the arch were much greater than the deformations that occurred for the completed arch. The strains in certain points in the FE model were compared with results obtained from strain gauges. The different construction events during the launching could clearly be seen in the strain results from the FE analysis even though they did not correspond exactly with field measurements.

Key words: bridge, assessment, FEM, load carrying capacity, evaluation, maintenance, ABAQUS, creep, viscoelasticity

Contents

Preface

This Master thesis was performed at the department of Civil and Environmental Engineering, Concrete Structures at Chalmers University of Technology in Gothenburg, Sweden. The work was carried out in the period between August 2004 and April 2005.

The main purpose of the Master thesis was to develop a Finite Element (FE) model of the New Svinesund Bridge, emphasis has been put on modelling the construction of the reinforced concrete arch. The work in this Master thesis was performed as a part of a research project called "Bridge Assessment and Maintenance based on Finite Element Structural Models and Field Measurements". This research project is performed in collaboration with The Royal Institute of Technology (KTH) and is financed by the Swedish road administration (Vägverket) and the Swedish railway administration (Banverket).

Our supervisor and examiner was Ph.D. Mario Plos at Concrete Structures, Chalmers University of Technology.

First we would like to thank and acknowledge Ph.D. Mario Plos for all assistance and constructive criticism throughout the progress of this Master thesis. We also want to thank the department of Structural Engineering and Mechanics, especially Prof. Björn Engström, Lic.Eng. John Eriksson, Ph.D Sigurdur Ormarsson for their support and valuable discussions. Furthermore we also want to express our gratitude to Anja Bäurich and Ralf Nitsche at Bilfinger Berger for their cooperation.

Finally, we want to express our gratefulness to our families and friends in Sweden, Montenegro and Portugal for their constant support and never ending faith in us.

Gothenburg April 2005

Senad Canovic and Joakim Goncalves

Notations

Roman upper case letters

A_c	Cross-sectional area of the concrete member
E_c	Modulus of elasticity for concrete
E_{cs}	Reduced modulus of elasticity
$E_{c,eff}$	Effective modulus of elasticity for concrete
$G_R(t)$	Time dependent shear relaxation modulus
G_0	Instantaneous shear relaxation modulus
$J_s(t)$	Shear compliance
$J_k(t)$	Bulk compliance
$K_R(t)$	Time dependent bulk relaxation modulus
K_0	Instantaneous bulk relaxation modulus
RH	Relative humidity

Roman lower case letters

f_{cm}	Mean compressive strength of concrete at 28 days
$f_{cm}(t_0)$	Mean compressive strength of concrete at time of loading, t_0
$g_R(t)$	Dimensionless shear relaxation modulus
h	Notional size of cross section
$j_s(t)$	Normalized shear compliance
$j_k(t)$	Normalized bulk compliance
$k_R(t)$	Dimensionless bulk relaxation modulus
p_0	Constant pressure
$\tilde{q}$	Uniaxial equivalent deviatoric stress
s	*C*oefficient which depends on the type of cement
t	Time
t_0	Time at initial loading of the concrete
u	Perimeter of the cross-section

Greek lower case letters

$\beta(f_{cm})$	Factor to take into account the effect of concrete strength on the notional creep coefficient
$\beta(t_0)$	Factor to take into account the effect of concrete age at loading on the notional creep coefficient
$\beta_c(t,t_0)$	Coefficient to describe the progress of creep with time after loading
$\beta_{cc}(t)$	Coefficient that depends on the age of concrete t in calculation of Young's modulus
$\beta_E(t)$	Coefficient that depends on the age of concrete t in calculation of Young's modulus
β_H	Coefficient depending on the relative humidity and the notional size of the concrete member

ε^{cr}	Creep strain
$\bar{\varepsilon}^{cr}$	Uniaxial equivalent creep strain
$\dot{\bar{\varepsilon}}^{cr}$	Uniaxial equivalent creep strain rate
$\varepsilon^{vol}(t)$	Total volumetric strain
$\varphi(t,t_0)$	Creep coefficient, defining creep at time t when loaded at age of concrete t_0
φ_0	Notional creep coefficient
φ_{RH}	Factor that takes the relative humidity into account when calculating the notional creep coefficient
γ	Shear strain
ν_0	Poisson's ratio
σ_c	Concrete stress
σ_0	Initial stress
$\Delta\sigma$	Stress difference
τ	Shear stress

1 Introduction

1.1 Background

A new road bridge, the New Svinesund Bridge at the border between Sweden and Norway, is now under construction and will be completed in the summer of 2005. The total length of the bridge is 704 m and it consists of a substructure in ordinary reinforced concrete together with a steel box-girder superstructure. The bridge has eight spans and the main span, with a length of 247 m across the border strait consists of a single arch in reinforced concrete, holding up the superstucture.

At the division of Structural Engineering, Concrete Structures, at Chalmers University of Technology, a research project is being carried out in order to improve on bridge assessment and maintenance of bridges through finite element (FE) analysis and field measurements. In this project, the New Svinesund Bridge is used as a case study.

During the construction of the bridge, a monitoring project is carried out in which the Royal Institute of Technology (KTH) is responsible for analysis and documentation, see James and Karoumi (2003). The results from this monitoring project will be used to evaluate results from the FE analysis and to update the FE model.

1.2 Aim and objectives

The FE model presented in this thesis was originally made for the bridge design. It was further on converted to the FE program ABAQUS by Mario Plos and Hamid Movaffaghi, see Plos and Movaffaghi (2004), as a part of the monitoring project. The aim with this thesis was to develop this FE model further, to include the long-term effects of the concrete in the arch and to model the sequential construction of the arch. The model was intended for calculation of deformations, sectional forces and moments as well as longitudinal stresses and strains. Strains obtained from the FE analysis was compared with the field measurements performed within the monitoring project in order to evaluate the modelling of the sequential construction especially. The main aim was to model the bridge so that the real structural behaviour was predicted in the FE analysis. Consequently, it was assumed that the material properties should be represented by mean values and not by characteristic or design values.

2 Bridge assessment and maintenance of bridges

Significant effort has been put into the development of new standards and codes in design of new structures in recent decades, but relatively little has been done in order to develop guides for bridge assessment on existing structures, see e.g COST 345 (2001). When the load-carrying capacity of existing bridges is evaluated, many bridges show insufficient capacity according to the current methods of bridge strength assessment. However, in reality, many bridges have a capacity reserve, which is not accounted for by these methods. This leads to great economical and environmental losses because many bridges are replaced or strengthened even though it is not necessary. Consequently, more correct bridge strength assessment is needed for the future.

2.1 Purpose of bridge assessment

During the existence of a bridge, many circumstances might change compared to what was assumed during the design of the bridge. Traffic loads might change and the state of the bridge changes due to deterioration and other external forces. In order to guarantee the safety and serviceability of the bridge, inspections and assessments are necessary.

When a bridge has deteriorated or been damaged it is in principle relatively simple to determine what type of repairs that are necessary. In the absence of a detailed bridge assessment the objective would be to restore the bridge to its original condition. However, when the bridge has no obvious problem but, for example, traffic loads have increased or maybe an aspect of the original design rules is outdated, it is very difficult to decide if safety measures are needed.

In this case, an assessment is required in order to see if the bridge is under unacceptable risk. If this is the case actions are needed in order to prevent failure. Consequently, bridges that are potentially in the risk category need to undergo bridge assessment in order to find out what precautions should be taken, if any.

A bridge that has been assessed and for which it has been shown that the state of the bridge is unsatisfactory won't necessarily collapse. However, if such a structure was left without any precautions taken, there would be an unacceptable risk that failure would happen during service.

2.2 The different stages in bridge assessment

In a bridge database, managed by the owner or the administrator of the bridge, the knowledge and history of each bridge is successively stored. This database is then used for future assessments of the bridge. The bridge assessment is based on the facts from design, construction and inspections of the bridge. Therefore, a typical bridge assessment is made after the bridge has been constructed, during the maintenance

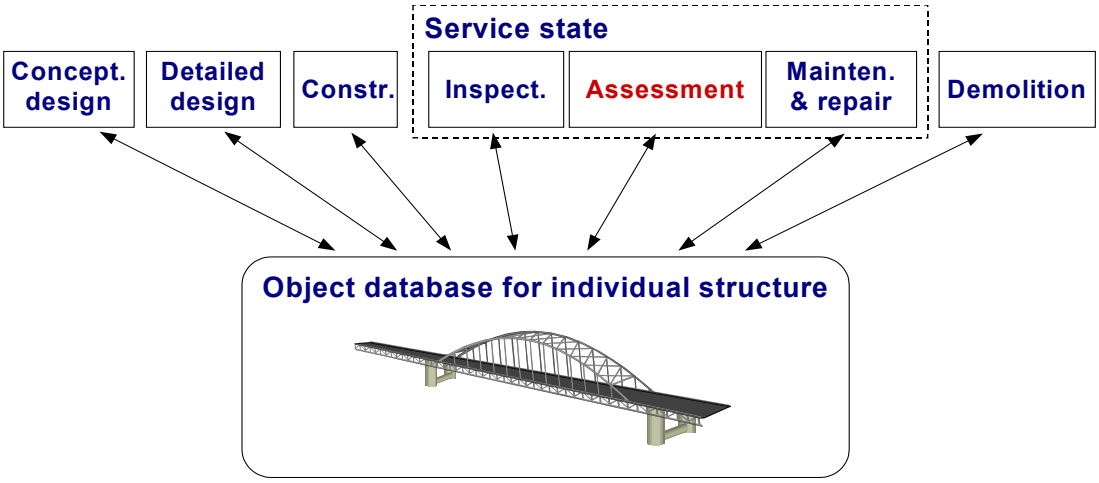

Figure 2.1 The different phases in the history of a bridge, showing the bridge assessment in its context. Figure adopted from Plos and Gylltoft (2002).

period, see figure 2.1. During the maintenance period there are three main activities according to Plos and Gylltoft (2002): inspections, assessments and repairs. The inspections are planned and are done regularly. Some repairs are also done regularly or are the outcome of an assessment.

There are different reasons for performing a bridge assessment and according to Plos and Gylltoft (2002) they can be divided in four main categories:

- **Changed demands** – Due to increased traffic loads and alterations in codes and regulations.
- **Planned reconstruction –** Reconstruction of a bridge often implies changes in the load carrying structure.
- **Damage** – The bridge might have been damaged due to external effects such as natural disasters, overloading, collisions, fire, etc.
- **Deterioration -** This can happen due to external environmental effects such as chloride penetration, corrosion, freeze-thaw splitting and carbonation. It can also appear due to internal reactions.

Bridge assessment can include more aspects than just strength calculations regarding risk of collapse. It can also include evaluation of function such as deformation, vibrations, cracking and the state with respect to deterioration.

In addition to analysis and calculations, other activities such as thorough inspections, testing and measurements and statistic evaluation of safety can be made. Depending on the outcome of the assessment it can result in different measures. These may consist of a simple verification of that the structure can fulfil the demands and no special measures need to be taken. If the demands are not fulfilled the structure might be strengthened, repaired or even replaced. In some cases an economical solution can be to decrease the allowed traffic load.

2.3 The different levels of structural analysis in bridge strength assessment

If ordinary design standards are used for assessing a bridge, the decisions made may easily become over-conservative. One reason for this is the fact that the codes for design have a greater safety margin than what is reasonable for assessment of existing bridges. The main reason for this is that the knowledge of an existing bridge far exceeds the knowledge of a bridge to be built, because of the possibilities to observe or measure the condition on the existing bridge. Often, more favourable values for material parameters and loads are found for the existing bridge compared with what was assumed in the design. Also, partial safety factors can be reduced and still the same structural safety can be achieved. However the choice of more adequate safety margins is complicated due to the lack of rules on how such a choice is made. One further reason why optimum safety levels are higher in design compared to assessment is the great cost coupled to improvement of an existing bridge.

Beyond the different safety levels that can be adapted there are also different levels of accuracy for the analysis models used, which can be chosen when performing a structural analysis in a bridge assessment. According to Plos and Gylltoft (2001), the different accuracy levels for the structural analysis can be defined in the following way.

The most common level for structural analysis is the "**standard level"** where only simplified linear calculations are done to determine sectional forces and sectional moments. Conventional design methods are used to check sections and details.

More accurate structure analysis can be performed with linear three dimensional (3D) finite element (FE) modelling to obtain sectional forces and sectional moments. Checking of critical parts or sections is then made with same methods as on "standard level". For concrete structures, analysis on this level has often given more unfavourable results than for conventional simple calculations. This is because linear calculations often lead to great stress concentrations that do not appear in reality. There are also certain effects in 3D analysis that are normally not taken into account, which increase the sectional forces and sectional moments. However, in cases where the response of the structure is mainly linear also in reality, a structural analysis on this level can be a great improvement.

In order to reflect the real structural behaviour, **advanced simulations** are needed in most cases. This requires non-linear FE analysis, where the material properties are modelled as non-linear. In this analysis the real material response such as cracking, yielding and failure is taken into account. These simulations usually require more work effort. Furthermore, analysis results from different load components cannot be superimposed. Therefore, such an analysis is performed using critical load combinations determined by simplified analysis. For failure modes that cannot be included, depending on the detailing of the models, such as shear failure and anchorage failure, conventional design methods are used. For this kind of analysis the outcome has generally been more favourable than for analysis performed on "standard level".

Simple analysis is obviously more cost effective and requires less work effort if it proves that the bridge is in a satisfactory condition but, if this can't be proven, more advanced analysis should be made in order to prevent unnecessary remedial actions and large economical losses.

2.4 Combining FE-analysis and field measurements

The reliability of a structural analysis depends on how well the structure, the material properties and the boundary conditions in a model coincide with reality. In order to verify the accuracy of the results, comparison with field measurements is suitable. Field measurements can also be used for updating the models and thereby making the models reflect reality better.

The field measurements can consist of dynamic loading, measurement of accelerations and modal analysis or static loading and measurement of e.g. deformations, strains or forces. With optimisation routines, the best possible adaptation of the sought parameters for the model can be done when the response under a specific load is known. With such methods, models that reflect the real structural response can be achieved for service loads. Updating the model for loads in the ultimate limit state is obviously not possible due to practical reasons. But a model that is well calibrated in the service state is generally more reliable also in the ultimate limit state.

2.5 Uncertainties in modelling

In bridge assessment as well as in design, the engineer has to deal with uncertainties due to variations in most variables such as material properties, loads and geometry. Other uncertainties are due to imperfect modelling and estimation errors. When assessing a bridge, the uncertainties can be reduced in comparison with design. The structure already exists and, for example, the loads and material properties can be measured, and the overall structure can be tested. Even when these measurements are done some uncertainties always remain in an assessment due to inherent variability, imperfect modelling and estimation error. The uncertainties due to inherent variability appear because certain phenomena are unpredictable, such as wind loads, material properties etc. These values can only be said to be within a certain range and with a certain probability to appear. These uncertainties can be taken into account with probabilistic methods.

3 Long-term effects for reinforced concrete

As the long-term effects are to be regarded in the analysis of the New Svinesund Bridge the time-dependent properties of the reinforced concrete should be taken into account. These are creep, relaxation and shrinkage of concrete, and also the development of Young's modulus in time. These properties are not only of interest in the long-term perspective but also in the short-term, during the construction of the bridge. In this thesis, emphasis has been made on the viscoelastic behaviour of concrete (creep and relaxation). In addition to the development of Young's modulus, the only long-term effect modeled was the creep and relaxation of concrete. Shrinkage was not taken into account in the model even though it could be of interest. In this chapter, the long-term effects of concrete are described as phenomena, basic equations are presented and the implementation of creep in the model is described.

3.1 Shrinkage

Drying of concrete in air results in shrinkage. If the concrete member is restrained, inner tensile stresses are developed when the volume decreases, which may cause cracks. Shrinkage is a time dependent deformation that is not affected by stresses acting on the concrete member. The major influences are the composition of the concrete, the member thickness and the relative humidity.

The total shrinkage strain is composed of the drying shrinkage strain and the autogenous shrinkage strain. The drying shrinkage strain is the strain developed due to the evaporation of the water through the hardened concrete. The autogenous shrinkage strain develops due to chemical reactions in the early days after casting, when the concrete is hardening; it should be considered especially when concrete is cast against already hardened concrete.

3.2 Creep and relaxation of concrete

Stress-dependent deformations can be divided into instantaneous and time-dependent deformations according to the Swedish "Concrete Handbook", see AB Svensk Byggtjänst (1994). The instantaneous deformations appear at the time of loading and if the load remains on the structure, the time-dependent deformations appear, the so-called creep. The deformations can also be divided into reversible and irreversible. The reversible instantaneous deformations are called elastic and the irreversible instantaneous deformations are called plastic. If the load remains the creep begins, in the beginning at a high rate and then the rate decreases with time, but the creeping never ends completely. The creep of concrete consists of a reversible and an irreversible part. The first part is called delayed elastic creep and the latter viscous creep. If the concrete is later unloaded, the recovery happens in a similar way through instantaneous (elastic) recovery and a time dependent delayed elastic recovery. Some permanent deformations remain after unloading due to plasticity and viscous creep. This so-called viscoelastic behaviour is schematically presented in figure 3.1.

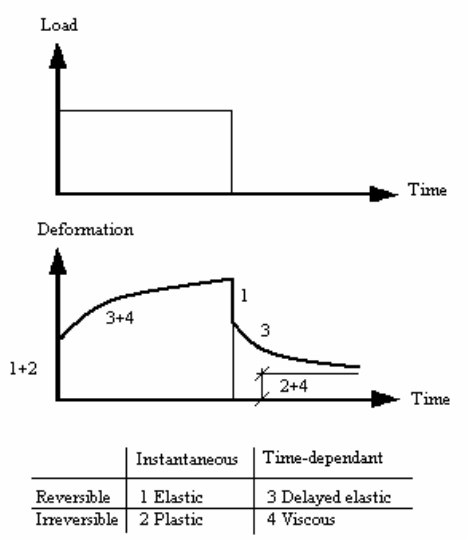

	Instantaneous	Time-dependant
Reversible	1 Elastic	3 Delayed elastic
Irreversible	2 Plastic	4 Viscous

Figure 3.1 Strain response for a constant load.

In general, the term creep is used if deformation increases with time under more or less constant stress. The creep is defined from a state of constant stress over time. Relaxation is basically the same phenomenon as creep, but the term is used for situations where the deformation is more or less constant due to constraints; here the stress decreases with time.

The creep and relaxation of concrete depends on the ambient humidity, the dimensions of the element, the composition of the concrete, age of concrete when first loaded and magnitude and duration of the load.

3.2.1 Calculation of the creep coefficient

The creep coefficient, $\varphi(t,t_0)$, is usually used to describe the magnitude of the creep deformations. It is defined as the total deformation (including creep) divided by the instantaneous deformation. When estimating the creep coefficient $\varphi(t,t_0)$ the parameters discussed above should be taken into account.

Calculation of the creep coefficient is made according to CEB-FIP Model Code 1990, see Comité Euro-International du Beton (1991). If the concrete is subjected to a compressive stress $|\sigma_c| < 0.4f_{cm}(t_0)$ at the concrete age at loading t_0, the following expressions for creep are valid. This is because it is reasonable to assume that creep is linearly related to stress within this range, concrete is then considered as an ageing linear viscoelastic material. In reality though, creep is a non-linear phenomenon, particularly if the stress exceeds $0.4f_{cm}(t_0)$.

The creep coefficient $\varphi(t,t_0)$ can be calculated from the following expression:

$$\varphi(t,t_0) = \varphi_0 \cdot \beta_c(t,t_0) \tag{1}$$

where φ_0 is the notional creep coefficient and
$\beta_c(t,t_0)$ is a coefficient that describes the progress of creep with time after loading.

The notional creep coefficient φ_0 is estimated from:

$$\varphi_0 = \varphi_{RH} \cdot \beta(f_{cm}) \cdot \beta(t_0) \tag{2}$$

where φ_{RH} is a factor that takes the relative humidity into account,
$\beta(f_{cm})$ is a factor to account for the effect of concrete strength and
$\beta(t_0)$ is a factor to account for the effect of concrete age at loading, t_0.

The factor φ_{RH} is calculated in the following way:

$$\varphi_{RH} = 1 + \frac{1 - RH/100}{0.46 \cdot (h/100)^3} \tag{3}$$

where RH is the relative humidity for the surrounding, expressed in percentage and
h is the notional size of the concrete member in mm, calculated as:

$$h = \frac{2 \cdot A_c}{u} \tag{4}$$

where A_c is the cross-sectional area of the concrete member and
u is the perimeter of the concrete member in contact with the surrounding atmosphere.

The factor $\beta(f_{cm})$ is calculated with the following expression:

$$\beta(f_{cm}) = \frac{5.3}{\sqrt{f_{cm}/10}} \tag{5}$$

where f_{cm} is the mean compressive strength of concrete, in MPa at the age of 28 days.

The factor $\beta(t_0)$ is expressed in the following way:

$$\beta(t_0) = \frac{1}{0.1 + t_0^{0.20}} \tag{6}$$

The coefficient $\beta_c(t,t_0)$ can be calculated using the following expression:

$$\beta_c(t,t_0) = \left[\frac{(t - t_0)}{\beta_H + (t - t_0)} \right]^{0.3} \tag{7}$$

where t is the age of concrete in days at the moment considered,
t_0 is the age of concrete in days when loaded and
β_H is a coefficient depending on the relative humidity and the notional size of the concrete member and is calculated with the following expression:

$$\beta_H = 1.5 \cdot \left(1 + \left(0.012 \cdot RH\right)^{18}\right) \cdot h + 250 \leq 1500 \tag{8}$$

According to CEB-FIP Model Code 1990, see Comité Euro-International du Beton (1991), the effect of the type of cement used and the effect of elevated or reduced temperature can be taken into account, but in this thesis those effects are considered negligible.

3.2.2 Methods to take creep into account in time dependent stress calculations

There are different models and methods to take creep into account in time dependent stress calculations. Three different major ways to take creep into account are here presented according to Cederwall (2000).

3.2.2.1 Effective modulus method (EM method)

In this model the Young's modulus, or modulus of elasticity for concrete is reduced through division by a factor $[1+\varphi(t,t_0)]$, so the effective modulus of elasticity becomes:

$$E_{c,eff} = \frac{E_c}{1+\varphi(t,t_0)} \tag{9}$$

This is a method in which the material can be seen as strain hardening, according to Cederwall (2000). This means that when the load changes the creep depends on the previously accumulated creep strains.

This method gives good results when the concrete stress does not vary significantly and when the aging of concrete is negligible, as for mature concrete. For varying stresses the results could be said not to be very satisfactory due to the fact that the creep deformation is estimated only on basis of final stress. So under increasing stresses the deformations are overestimated and for decreasing stresses the deformations are underestimated. This method is still used extensively for predicting creep deflections under permanent loads of reinforced concrete beams and to calculate the effect of creep in slender columns.

3.2.2.2 Rate of creep method (RC method)

This method is based on the assumption that the rate of creep is independent of the age at loading. The difference in strain that follows from a stress change is only dependent on the lapse of time from the first loading. Such a material can be classified as time hardening. It is then enough to know only one creep curve, the one for the first load applied. The figure below and equation (10) shows how the strains are calculated.

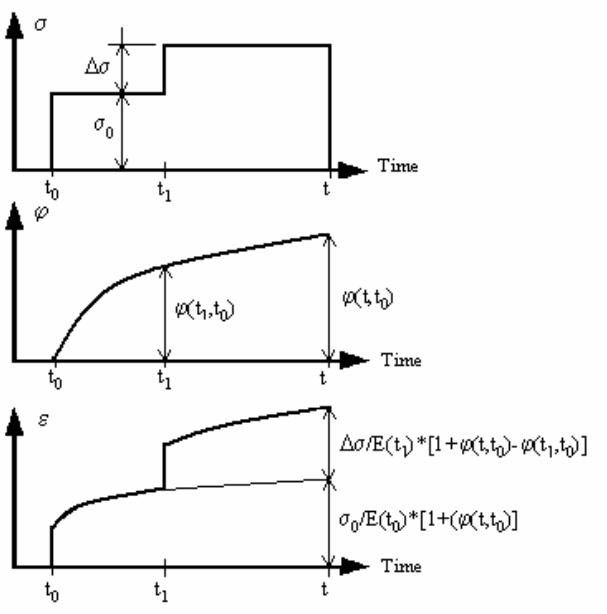

Figure 3.2 Principle on how strains are calculated with RC method.

$$\varepsilon(t) = \frac{\sigma_0}{E(t_0)} \cdot \left[1 + \varphi(t,t_0)\right] + \frac{\Delta\sigma}{E(t_1)} \cdot \left[1 + \varphi(t,t_0) - \varphi(t_1,t_0)\right] \tag{10}$$

This method underestimates the deformations when concrete is subjected to increasing loads. It can also be observed that this method takes into account the maturing of the concrete. So if both previous methods (EM method and RC method) are used, it is possible to calculate within what range the deformations are.

3.2.2.3 Method of Superposition

Concrete is a material that can be classified as somewhere in between strain hardening and time hardening. The method of superposition can be said to be somewhere in between these methods and is therefore applicable to concrete. If the stress varies from one stress level to another, two different creep curves for the different ages at loading t_0 need to be calculated. The two curves are as, the name of the method suggests, then superposed. The principle of this method is presented in figure 3.3 and the formula for calculating the strains is shown in equation (11).

$$\varepsilon(t) = \frac{\sigma_0}{E(t_0)} \cdot \left[1 + \varphi(t,t_0)\right] + \frac{\Delta\sigma}{E(t_1)} \cdot \left[1 + \varphi(t,t_1)\right] \tag{11}$$

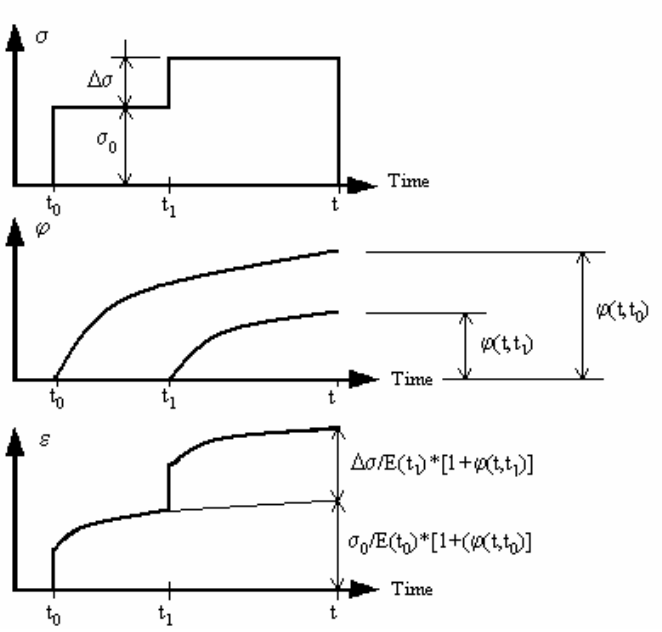

Figure 3.3 The principle of how strains are calculated with the superposition method.

3.2.3 Implementation of creep in ABAQUS with *CREEP

In order to model the creep behaviour of concrete in ABAQUS, the FE program used, see Hibbit, Karlsson and Sorensen Inc (2002), the option *CREEP was chosen in the material specification. Two different creep laws can be chosen in ABAQUS: the power-law and the hyperbolic-sine law. The hyperbolic sine law was rejected due to its difficulty and the power law was tried due to its comprehendible form. The power-law model can be used with either time hardening or strain hardening. According to Hibbit, Karlson and Sorensen Inc. (2002), the strain hardening form should be used when the stress state varies during analysis. The analytical expressions for time hardening and strain hardening are, respectively:

$$\dot{\bar{\varepsilon}}^{cr} = A \cdot \tilde{q}^{n} \cdot t^{m} \tag{12}$$

$$\dot{\bar{\varepsilon}}^{cr} = \left(A \cdot \tilde{q}^{n} \cdot \left[(m+1) \cdot \bar{\varepsilon}^{cr} \right]^{m} \right)^{\frac{1}{m+1}} \tag{13}$$

where $\dot{\bar{\varepsilon}}^{cr}$ is the uniaxial equivalent creep strain rate,
$\tilde{q}$ is the uniaxial equivalent deviatoric stress,
t is the total time,
$\bar{\varepsilon}^{cr}$ is the uniaxial equivalent creep strain and
A, n, m are user defined parameters.

Both of the above mentioned forms were analysed in a simple model to verify if any of them were applicable in the model for the New Svinesund Bridge. Description of the simple model and analysis of the results with regard taken to the theory in chapter 3.1 follows.

In order to obtain the correct values for A, n and m in the analytical expressions above, equation (12) was integrated with respect to time and the following equation was obtained:

$$\bar{\varepsilon}^{cr}(t) = A \cdot \tilde{q}^{n} \cdot \frac{t^{m+1}}{m+1} \tag{14}$$

This equation was then compared to the equation for creep strains:

$$\varepsilon^{cr}(t) = \frac{\sigma \cdot \varphi(t, t_0)}{E_c} \tag{15}$$

After many different attempts in Matlab, the values for A, n and m could be determined in order to represent the creep coefficient $\varphi(t, t_0)$.

The simple structure consisted of a one-dimensional concrete bar that was axially loaded. It was in the ABAQUS analysis subjected to the stress history in figure 3.4.

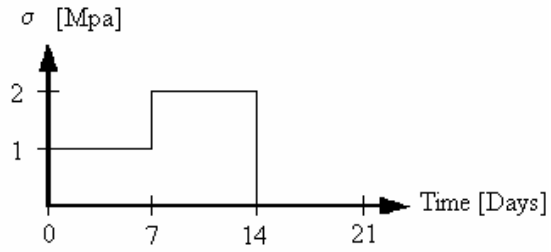

Figure 3.4 Stress history for the simple model in ABAQUS.

Depending on if time hardening or strain hardening was used in the creep definition, the results from ABAQUS were different. They are presented in principle in figure 3.5.

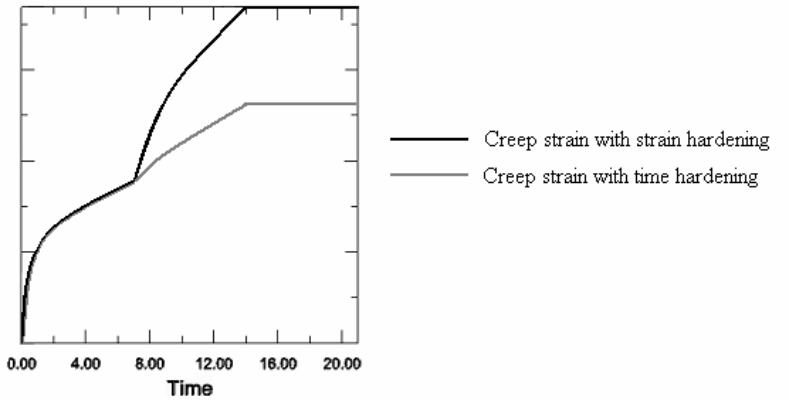

Figure 3.5 Creep strains from ABAQUS with time hardening and strain hardening.

By observing the results, some conclusions could be made about these two methods. The differences between the two models appear after the change of stress. For the model with time hardening, the additional creep strain, after the change of stress at time t_1, is the same as for a corresponding specimen, loaded with the higher stress level from the start, during the same time period, see figure 3.6. For the model with strain hardening, the additional creep strain after the change of stress at time t_1, is the same as for the corresponding specimen for the time period after it had reached the same creep strain level.

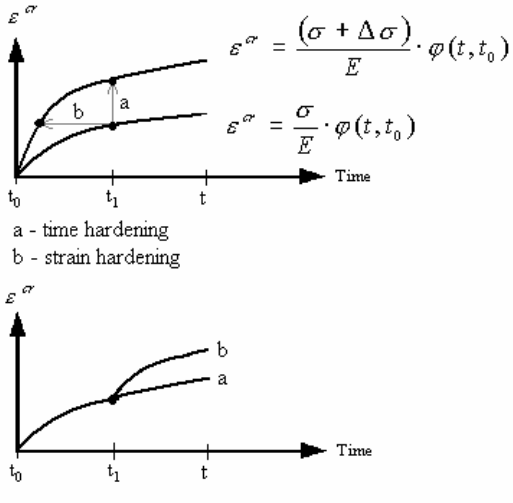

Figure 3.6 Difference of creep in ABAQUS with time and strain hardening.

There can be seen certain similarities between the time hardening form and the strain hardening form compared to the EM method and the RC method respectively, although the methods are not identical. However, concrete is a material with characteristics that are somewhere in between these methods. A method, which is more similar to the method of superposition, would be more suitable. The other major observation that can be made is that when the concrete is unloaded no decrease in creep strains appears. This is also not the case for concrete, which has been explained earlier in this chapter. Consequently, the conclusion that can be made is that the command *CREEP in ABAQUS is not suitable for analysis of concrete when the stresses vary, in particular not when the stress history involves unloading.

3.2.4 Time domain viscoelasticity in ABAQUS

In order to model the creep and relaxation of concrete in ABAQUS in a more accurate manner the material was modelled as viscoelastic in the time domain. In ABAQUS, a viscoelastic material is defined by a so called Prony series expansion of the dimensionless shear relaxation modulus $g_R(t)$ and the dimensionless bulk relaxation modulus $k_R(t)$, see Hibbit, Karlson and Sorensen Inc. (2002):

$$g_R(t) = 1 - \sum_{i=1}^{N} \overline{g}_i^P (1 - e^{-t/\tau_i^G}) \tag{16}$$

$$k_R(t) = 1 - \sum_{i=1}^{N} \bar{k}_i^P (1 - e^{-t/\tau_i^k}) \tag{17}$$

where N, $\bar{g}_i^P$, τ_i^G, $\bar{k}_i^P$ and τ_i^k are material constants and
t is the time.

The dimensionless shear relaxation modulus $g_R(t)$ and the dimensionless bulk relaxation modulus $k_R(t)$ are defined in the following way:

$$g_R(t) = G_R(t) / G_0 \tag{18}$$

$$k_R(t) = K_R(t) / K_0 \tag{19}$$

$G_R(t)$ and $K_R(t)$ are the time dependent shear relaxation modulus and bulk relaxation modulus respectively and they are obtained, for linear elastic materials, by multiplying the instantaneous relaxation moduli with some dimensionless relaxation function. Whereas, $G_0=G_R(0)$ and $K_0=K_R(0)$ are the instantaneous relaxation moduli, defined according to:

$$G_0 = \frac{E_0}{2 \cdot (1 + \nu_0)} \tag{20}$$

$$K_0 = \frac{E_0}{3 \cdot (1 - 2\nu_0)} \tag{21}$$

where ν_0 is Poisson's ratio.

In ABAQUS, the relaxation parameters can be defined in three different ways in the time domain. These are: direct specification of the Prony series parameters, specification of data from creep test or specification of data from relaxation test.

When direct specification of the Prony series parameters is chosen, the following material constants need to be specified: $\bar{g}_i^P$, $\bar{k}_i^P$ and τ_i. The number of terms specified in the Prony series is optional.

If creep test data are available, ABAQUS requires input of the normalized shear compliance and, if necessary, also the bulk compliance. These are defined in the following way:

$$j_S(t) = G_0 \cdot J_S(t) \tag{22}$$

$$j_K(t) = K_0 \cdot J_K(t) \tag{23}$$

where $J_S(t) = \gamma(t) / \tau_0$ is the shear compliance and $J_K(t) = \varepsilon^{vol}(t) / p_0$ is the bulk compliance. $\gamma(t)$ is the total shear strain, τ_0 is the constant applied shear stress, $\varepsilon^{vol}(t)$ is the total volumetric strain and p_0 is the constant pressure applied.

ABAQUS will then calculate the Prony series parameters by first converting the creep test data to relaxation data and then the shear relaxation modulus $g_r(t)$ and the bulk relaxation modulus $k_r(t)$ is used in a non-linear least-squares fit to determine the Prony series parameters.

When relaxation test data is available, the normalized shear and bulk moduli are directly defined and through a non-linear least-squares fit the Prony series parameters are calculated.

3.2.5 Implementation of creep in ABAQUS with relaxation test data

In order to model the creep behaviour of concrete in ABAQUS, specification of relaxation test data was considered to be the most suitable way. As described above, ABAQUS then requires the normalized shear and/or bulk moduli, $g_r(t)$ and $k_r(t)$, as function of time. Both these moduli where applied in the material definition with the ABAQUS command *COMBINED TEST DATA. With the purpose of implementing the creep coefficient, $\varphi(t,t_0)$, the normalized relaxation moduli had to be given as a function of the creep coefficient. The normalized relaxation moduli were then interpreted as follows:

$$g_r(t) = \frac{G_R(t)}{G_0} = \frac{\dfrac{E_0}{2\cdot(1+\nu_0)\cdot(1+\varphi(t,t_0))}}{\dfrac{E_0}{2\cdot(1+\nu_0)}} = \frac{1}{(1+\varphi(t,t_0))} \tag{24}$$

$$k_r(t) = \frac{K_R(t)}{K_0} = \frac{\dfrac{E_0}{3\cdot(1-2\nu_0)\cdot(1+\varphi(t,t_0))}}{\dfrac{E_0}{3\cdot(1-2\nu_0)}} = \frac{1}{(1+\varphi(t,t_0))} \tag{25}$$

In equation (24) and (25), $G_R(t)$ and $K_R(t)$ are the time dependent shear relaxation modulus and bulk relaxation modulus, and they are obtained by multiplying the instantaneous relaxation moduli with some dimensionless relaxation function. This dimensionless relaxation function was chosen as $1/(1+\varphi(t.t_0))$, which is then also the solution to how the normalized relaxation moduli are expressed as function of the creep coefficient. It can also be said that Poisson's ratio is assumed to be constant in time. The values for $g_r(t)$ and $k_r(t)$ are then inserted into ABAQUS for different time steps, see Appendix A. Through the non-linear least-squares fit, the Prony series parameters are calculated.

In order to verify that this method gives reasonable results, the same simple structure as mentioned in chapter 3.3 was subjected to the same stress history, which can be seen in figure 3.4. The results from the FE-analysis in ABAQUS were compared to calculations made in MATLAB. The calculations made in MATLAB were based on the method of superposition, which is a method suitable for calculation of creep in concrete, see Appendix B for the input file used in MATLAB. The creep strains obtained from both analyses were compared and are shown in figure 3.7.

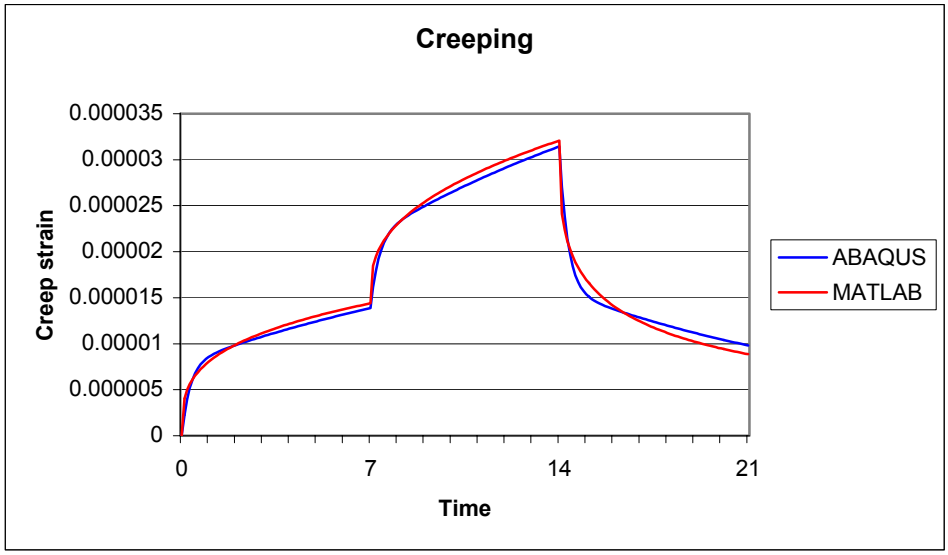

Figure 3.7 Creep strains obtained from the ABAQUS and the MATLAB analyses.

As can be seen in figure 3.7, the creep strain obtained from ABAQUS coincide reasonably well with the creep strain calculated in MATLAB. The small differences that appear could be due to the chosen discrete input values used for the *COMBINED TEST DATA and due to the least-squares fit made in order to convert the normalized relaxation moduli to the Prony series expansion. It could also be seen in ABAQUS that when the analysis was made over long time the creep recovery after unloading was complete and the creep strains eventually decreased to approximately zero.

The conclusion is that this model is very similar to the method of superposition. On the other hand, it has no irreversible parts, neither plastic nor viscous. For concrete in reality, this is not the case. Still, this way of modelling was considered to be appropriate for the concrete in the FE model and was therefore used.

3.3 Development of Young's modulus

In the construction process of the New Svinesund Bridge, the concrete is loaded at an early age when the concrete has not matured significantly. Consequently, the development of Young's modulus was taken into account in the FE model. The maturing of concrete, which is the development of strength and stiffness with time, is a process due to chemical reactions in the material. In the beginning the maturing rate is high and it gradually decreases to a very low rate, although the maturing of concrete never ends completely.

Calculation of Young's modulus was made according to CEB-FIP Model Code 1990, see Comité Euro-International du Beton (1991). The strength of concrete used in the arch was known due to sample tests made, see FB Centrallaboratorium (2004). The mean value for the compressive strength from the different tests was calculated, and from that value the modulus of elasticity can be estimated:

$$E_c = \alpha_E \cdot (f_{cm} / f_{cm0})^{1/3} \tag{26}$$

where E_c is the modulus of elasticity at a concrete age of 28 days (MPa),
α_E =2.15*10^4 (MPa),
f_{cm} is the compressive strength of concrete at an age of 28 days (MPa) and
f_{cm0} =10 (MPa).

When only an elastic analysis is made, a reduced value for the modulus of elasticity should be used in order to account for initial plastic strain:

$$E_{cs} = 0.85 \cdot E_c \tag{27}$$

where E_{cs} is the secant modulus of elasticity in the elastic range for concrete.

In order to account for an age of concrete different than 28 days, the following equation can be used:

$$E_c(t) = \beta_E(t) \cdot E_{cs} \tag{28}$$

where,

$$\beta_E(t) = (\beta_{cc}(t))^{0.5} \tag{29}$$

and where,

$$\beta_{cc}(t) = e^{s\left(1-\left(\frac{28}{t/t_1}\right)^{0.5}\right)} \tag{30}$$

where $\beta_E(t)$ and $\beta_{cc}(t)$ are coefficients which depend on the age of concrete t,
t is age of concrete (days),
t_1=1 day and
s is coefficient which depends on the type of cement used.

In this way the development of Young's modulus was calculated in MATLAB, see Appendix C. The results achieved can be seen in figure 5.3, section 5.1.4. According to CEB-FIP Model Code 1990, see Comité Euro-International du Beton (1991), effects due to reduced or elevated temperature can be taken into account when estimating Young's modulus. However, this effect was not taken into account in this thesis.

4 The New Svinesund Bridge

4.1 Description of the bridge

The New Svinesund Bridge between Sweden and Norway is currently being constructed and is planned to open for traffic in the summer of 2005. It is being built on behalf of the Swedish and Norwegian road administrations, Vägverket and Statens vegvesen respectively. The main contractor is Bilfinger Berger AG. The New Svinesund Bridge is a highway bridge across the Ide Fjord. The total length of the bridge is 704 m and it consists of a substructure in ordinary reinforced concrete together with a steel box-girder superstructure. The bridge has eight spans and the main span consists of a single arch in reinforced concrete with a span of 247 m across the strait, see Figure 4.1. The arch is very slender due to the esthetical demands and it has the greatest span in the world for a bridge of this type. Consequently, advanced technical solutions have been used in order to complete the sequential construction of the arch.

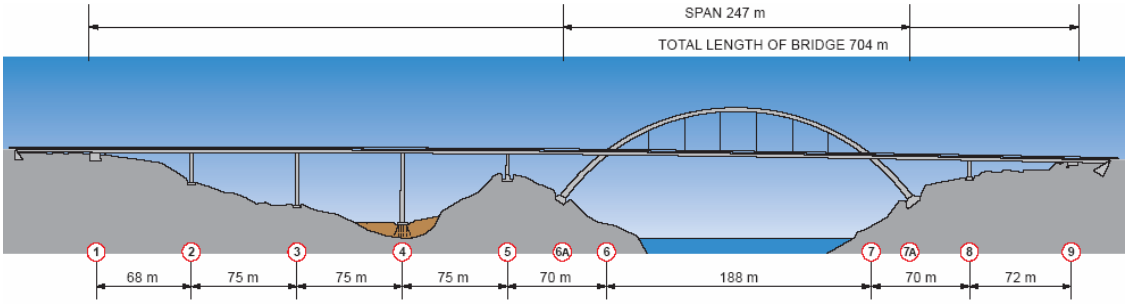

Figure 4.1 Drawing of the New Svinesund Bridge showing the spans and their lengths. Figure from www.vv.se/svinesundsforbindelsen.

4.1.1 The arch

The arch has an approximately rectangular hollow section that tapers in both width, height and wall thickness from the abutments to the crown, see figure 4.2. The section at the abutments is approximately 6.2 m wide and 4.2 m high with wall thickness of 1.5 m and 1.1 m, respectively. Close to the crown the section is approximately 4 m wide and 2.7 m high with wall thickness of 0.6 m and 0.45 m. The arch rises from a level of approximately +28.3 m at the abutments to a level of +91.7 at the crown. The bridge decks connect with the arch at about half of its height, at approximately +59.9 m.

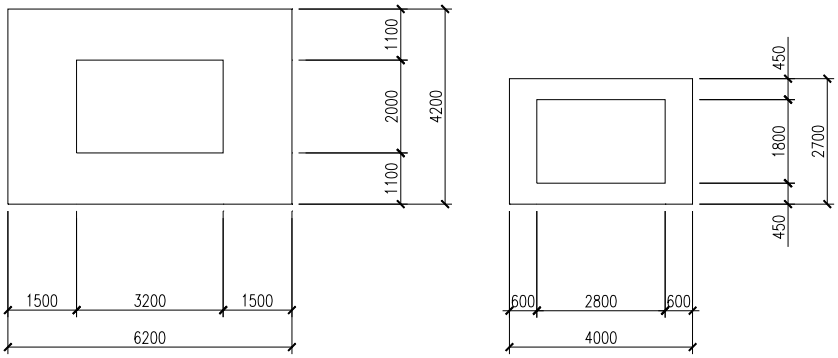

Figure 4.2 Cross-sections of the arch at the abutment (left) and near the crown (right).

The arch is made of reinforced cast-in-situ concrete with concrete class K70, which is produced in Strömstad (Sweden) and Halden (Norway). Two different classes of reinforcement bars were used, K 500 and Ks 60 S, see Appendix D for the material properties for concrete and reinforcement.

4.1.2 The bridge decks

The arch carries two steel box-girder bridge decks, one on each side, which provides the bridge with a total width of approximately 28 metres. Each bridge deck is composed of two five and a half metres wide and 24 metres long prefabricated steel elements that are welded together on site to produce the ten-metres wide decks, see figure 4.3. The steel plates of the box-girder sections are stiffened with longitudinal profiles. The arch is joined to the bridge decks through stiff connections at the intersections. This assists to give lateral stability to the arch. Between these intersections, where the arch rises above the bridge decks, traverse beams positioned with 25.5 m intervals join the two bridge decks. These traverse beams are in turn supported by hangers to the concrete arch. In total there are six pairs of hangers that support the bridge decks. For the land spans, columns and abutments support traverse beams between the bridge decks. The eight metres wide and three metres high traverse beams are anchored to the supports through cables that are fixed to clamping struts inside the supports, see Figure 4.3.

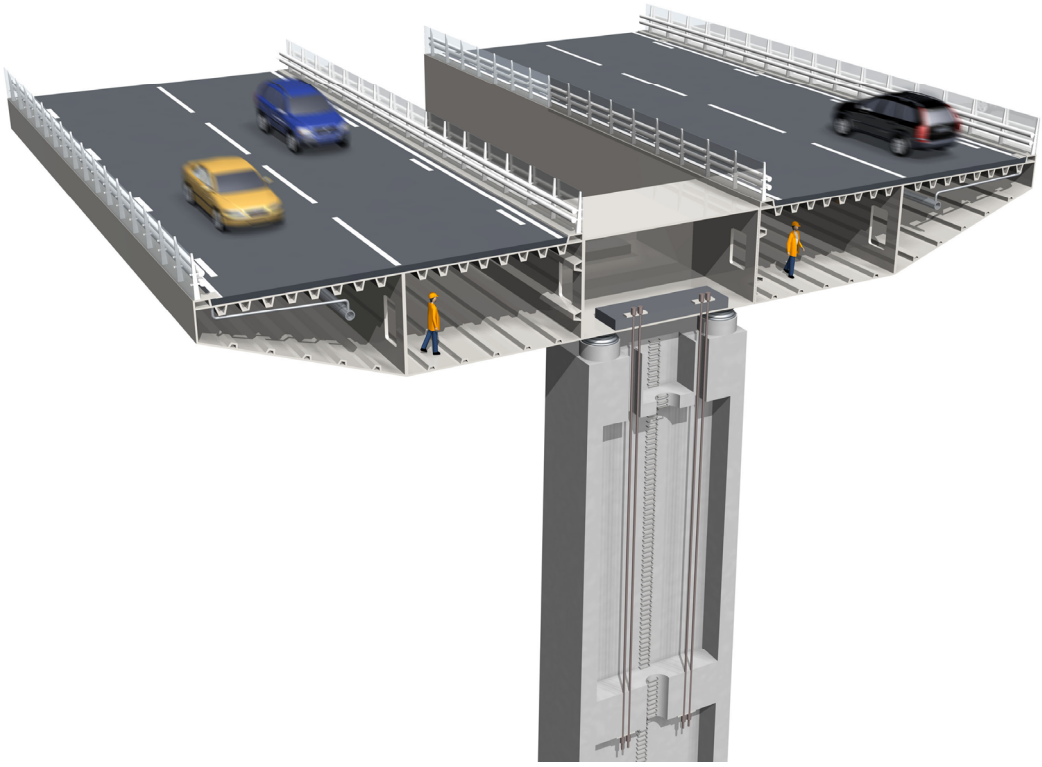

Figure 4.3 Cross section of the bridge decks with a transverse beam supported by a column. Figure from www.vv.se/svinesundsforbindelsen.

4.1.3 The foundation

The superstructure of the bridge is supported by two land embedments, five intermediate column supports and the main span is suspended in the arch, see Figure 4.1. The substructure is made of reinforced concrete, concrete class K40. Eight of the nine supports have rock foundation where the base plates are cast in shallow shafts that were blasted in the rock. One of the supports is located in a peat bog and the foundation here consists of steel core piles driven into the ground. The lengths of the piles vary between 9 and 16 metres and the diameter is approximately 14 cm. As the landscape near the bridge has large differences in levels the supporting columns vary extensively in height, between 11 and 47 metres.

4.2 Construction of the bridge

It was planned that the construction of the bridge would be carried out in a short and intensive period of 36 months, including the technical preparations. The bridge will be finished in the year of 2005. During 2003, the construction of the arch, the piers and the superstructure on the southern side was the main work. In 2004, the superstructure was finished together with all the construction work connected to the arch. And at last, all remaining work, including the surfacing, will be finished in the spring of 2005.

4.2.1 Construction of the arch

The work on constructing the arch was carried out simultaneously on both sides of the fjord and the arch halves were finally linked together in the middle of the arch. On the Swedish side, the work on constructing the arch started the 15:th of May 2003, a whole month before the work on the Norwegian side. The Norwegian side was able to reach the same level in the working schedule in September, when the Swedish side had paused the work for a month. Hereafter, the development on both sides was in general similar. The construction of the arch was made using a technique of climbing formwork and the cantilever construction method with temporary cable–stayed supporting, see Figure 4.4.

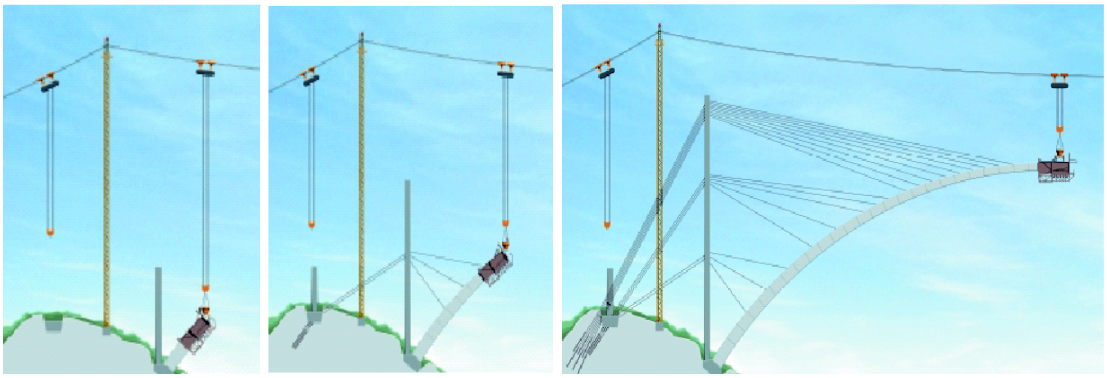

Figure 4.4 Drawing showing the launching of the arch and its temporary support. Figure from www.vv.se/svinesundsforbindelsen.

The first thing to be produced was the foundation of the arch. Then, the first segment on each side was cast using traditional scaffolding for the mould. After this, the following 48 arch segments (i.e. 24 arch segments from each side) were cast using the self-climbing formwork. To hold the segments in position, supporting cables were used. Finally, the crown segment was cast to link the two halves together, completing the arch. In order to be able to dismount the temporary supports, steel pressure bars were cast into the crown segment. It was calculated when scheduling the work that one work cycle on a segment, moving the mould and reinforcing and casting the concrete, should take approximately one week for around 15 workingmen. In reality the work cycle for the first 9 segments took two weeks and the following segments had a work cycle that took one week as scheduled, see Appendix E.

When casting the arch segments, they deflected from their original casting position due to their self-weight. With calculations, it was possible to predict these deformations. This information was used when planning the casting procedures so that the arch would get the final form it was designed to have. The solution was to cast the segment with a larger angle to the horizontal plane than the final. Hence, after deformation, the segment would end up in the correct position. In addition to this, adjustments of the force in the supporting cables were used to correct the position of the arch.

The system of climbing formwork, which was used for casting of the arch segments, had a hydraulic self-climbing casting mould that was anchored to the previous arch segment. The anchorage was released when casting of the segment was completed. Then, the climbing formwork was moved forward and adjusted so that the

preparations of casting the next segment could be done. These preparations included the positioning and completion of a pre-fabricated reinforcement cage in the formwork, installation of the supporting cables, if such were needed, and completing the formwork.

Instead of conventional cranes a cable conveyor that was mounted across the fjord was used for transporting material for the arch, see figure 4.4. The cable towers were made of trusses and could be angled ±10 metres laterally to be able to serve the entire arch width. The material was carried in motorized carriages that ran along the cable that was connected to the truss towers on each side of the fjord.

The concrete was loaded into what is known as a concrete skip, which can lift up to 7000 kg. The bottom of the skip opened when it reached the mould and the concrete was poured through casting hatches on the upper edge of the mould and was vibrated. For completing of one segment, approximately 60 m^3 of concrete was needed. This requires approximately 144 000 kg of concrete. Consequently, the concrete skip needed to deliver at least 21 times per segment.

4.2.2 Temporary supports

When constructing the arch, very high moments would act on it and, consequently, high tensile forces would occur in the concrete if temporary supports were not used. Temporary towers were built behind each cantilevering half to act as auxiliary supports. The arch cantilevers were supported by cables connected to the temporary towers, see figure 4.4. The towers were in turn supported by cables fixed to rock anchors. When the arch was finished these temporary supports were removed.

The towers were made of reinforced concrete, concrete class K45. Conventional climbing formwork was used for the casting of the towers, that were constructed in stages, as can be seen in figure 4.4. The towers reached 112 metres above sea level, standing on foundations behind the arch and they had a square box cross-section. The cables that held the arch segments went through the concrete tower and were anchored to the back of it. The cables that stabilized the tower went from the front trough the tower and were anchored in the rock. The cables were anchored to the towers on three anchorage levels.

For the first 12 segments, a new pair of cables was installed only every second segment, but for the following 13 segments there was a new pair of cables installed in each segment. The cables were made of steel and one cable consisted of several strands. During the construction, it was possible to adjust the tensile force in the cable or to cut off some of the strands to decrease the cross-section area.

Depending on if a segment should have a pair of supporting cables or not, the construction procedure of the segment was different. If there were no new cables installed, an increase of the tensile force in the last installed pair of cables was made by additional post-tensioning.

In order to provide transverse stability during the construction of the arch, a pair of inclined transverse cables was installed in arch segment 15. One cable on each side of

the arch cantilever was anchored to the rock beside the arch foundations. When the arch was completed and the bridge decks were launched, these transverse cables were removed.

4.2.3 Construction of the superstructure

The superstructure was constructed in sections and assembled together afterwards. The construction site for the superstructure sections was in Germany and they were transported by sea from Rostock. The assembly method used for the superstructure was different on the Swedish side compared to the Norwegian side. There is also a longer part of the superstructure on the Swedish side, see figure 4.1.

The assembly method used on the Swedish side was to weld the sections together and then launch the bridge deck out over the bridge supports, using hydraulic jacks. The jacks were able to push 0.5 m each time and the structure was pushed at a level of 0.5 m above the final level. Finally, when the entire structure had reached its position, it was lowered to its final level on the pier abutments.

On the Norwegian side a more conservative method was used were the sections were welded together directly in their final position, while they were resting on a fixed scaffold.

When assembling the sections that connect supports 5 and 6 on the Swedish side and supports 7 and 8 on the Norwegian side, see figure 4.1, the sections were welded together in their final position held by a large crane.

The last part that was installed was the central section of the bridge deck that is suspended from the arch. The central section was welded together in Halden harbour. It was then transported by sea on barges to the bridge site were it was lifted by jacks mounted on temporary cables hanging from the arch. When the final position was reached the section was connected to the permanent pairs of hangers from the arch and to the rest of the bridge deck.

4.3 Field measurements on the bridge

The New Svinesund Bridge is a structurally complicated bridge. In order to learn more about the structure, the bridge project manager, the Swedish road administration (Vägverket), initiated a monitoring project. The Norwegian Geotechnical Institute (NGI) is responsible for the measurements and the Royal Institute of Technology (KTH) is responsible for analysis and documentation in this project. This monitoring project includes field measurements to be conducted during the construction phase, testing phase and the first years of operation. According to James and Karoumi (2003), the primary aims and objectives for these field measurements are to check that the bridge is built as designed and to learn more about the actual structural behaviour of the bridge, compared with that predicted by theory. In this Master Thesis, the results of the field measurements are used for comparison with analysis results.

4.3.1 Description of sensors

Within the monitoring project strains in critical sections of the arch are measured. Two different types of strain gauges were installed for the measurement of the internal strains within the box section of the concrete arch; these are the vibrating wire strain gauge and the resistance strain gauge. Both of these sensor types are preassembled on normal reinforcement bars, so-called sister bars, and placed alongside the main reinforcement. The sensors are embedded in the concrete and the lengths of the bars are such that full bonding with the concrete can be accomplished at both ends of the bars.

A total of 28 temperature gauges were installed in order to measure the temperature within the concrete arch. The air temperature is also monitored with a separate temperature gauge installed as part of the SMHI (Swedish Meteorological and Hydrological Institute) wind monitoring system. This system also has a wind speed and direction gauge and was installed by SMHI prior to beginning the construction work on the bridge. It was later moved closer to the bridge.

In order to measure accelerations in the concrete arch two instrument boxes with two accelerometers in each were mounted within the hollow cross-section of the arch. One accelerometer was oriented vertically and the other horizontally; measurements were made in the same directions. During the construction phase, the two boxes with accelerometers were moved a couple of times towards the centre of the bridge. When the arch was completed the instrument boxes were moved to their final position, i.e. one at the midpoint and one at the Swedish quarter point of the arch.

In addition to the measurements in the monitoring project, the contractor Bilfinger Berger AG measured the prestressing forces in the temporary support structures. The geometry of the arch was also measured during construction in order to control the deformations.

4.3.2 Location of strain gauges

Of the above mentioned field measurements, it is the results obtained from the strain gauges that was compared with the results from the FE analysis. Therefore it is of interest to know the position of these gauges and the nomenclature used to identify each sensor. The first part in the sensor nomenclature is used in order to describe the type of sensor. For the strain gauges it is **VW** for the **V**ibrating **W**ire strain gauge and **RS** for the **R**esistance **S**train gauge. The next part in the sensor nomenclature is used to identify if the sensor is on the **S**wedish or **N**orwegian half of the arch and is described with the letter **S** or **N**. The number following this letter describes in which segment the sensor lies. Furthermore, the nomenclature also has a letter to describe the position within the segment. The following letters are used for describing the position within the segment:

T = **T**op wall of the arch
B = **B**ottom wall of the arch
E = **E**ast wall of the arch
W = **W**est wall of the arch

A typical example is the sensor **RSN6-T,** which is a **R**esistance **S**train gauge situated in segment **6** on the **N**orwegian side in the **T**op wall of the segment.

Table 4.1 Total number and location of the strain gauges.

Sensor	Number	Location
Vibrating wire strain gauge (VW)	16	4 in S1, 4 in S6, 4 in N1, 4 in N6
Resistance strain gauge (RS)	8	2 in S1, 2 in N6, 4 in S25

In Table 4.1, the type and total amount of strain gauges used in the monitoring programme can be seen. All sensors including the strain gauges are positioned as close as possible to the longitudinal or transverse axis of symmetry within the segment. The strain gauges are installed in the outer main reinforcement layer. For more detailed information about position of strain gauges see James and Karoumi (2003).

5 Finite element model

The finite element (FE) model of the New Svinesund Bridge, used in this thesis, is described below. The FE model was based on the FE model produced by Mario Plos and Hamid Movaffaghi, see Plos and Movaffaghi (2004). The authors also produced a simplified analysis of the launching of the bridge arch. In this thesis, the model was further developed for the analysis of the bridge launching. Modifications of the model were made and a detailed analysis of the launching of the arch and the completion of the bridge was performed. The main modifications, in addition to a more detailed modelling of the launching of the arch, were to introduce the development of Young's modulus with time, modelling the viscoelastic behaviour of material to take the effect of creep into account and to include the temperature load on the structure.

The FE model of Plos and Movaffaghi was based on the structural model produced by the bridge contractor, Bilfinger Berger (2004). Bilfinger Berger supported with some of their indata files for the model, used in the design of the bridge, and with design and construction documents. The indata files were converted and adopted to the general purpose FE program ABAQUS, see Hibbit, Karlsson and Sorensen Inc. (2002).

5.1 Description of the FE model in ABAQUS

5.1.1 General

The FE-model was generated and analysed in the finite element program ABAQUS, see Hibbit, Karlsson and Sorensen Inc. (2002). In ABAQUS, the finite element analysis requested is described by an input file. In this thesis, the input file was created by using a text editor. The input file was divided in two parts, model data and history data.

Model data specifies the finite element model, including the geometry and the material of the finite element model. This means defining the elements, the nodes, the element properties, the material definitions, the boundary conditions and any data that specifies the model itself.

History data is the actual analysis part and it describes what happens to the model in time. The history data can be divided into several sequential steps and there is no limit on the number of steps in an analysis. Within a step it is defined what type of analysis is performed, what happens to the model, e.g. loading or any change of the model, and the outdata that is requested. Control parameters for time integration and loading are also defined. Steps are introduced to make modifications of these parameters or to change the geometry for example.

5.1.2 Geometry

The geometry in a model is represented with nodes and elements. The elements connect the nodes to each other and a structure is built up, see figure 5.1.

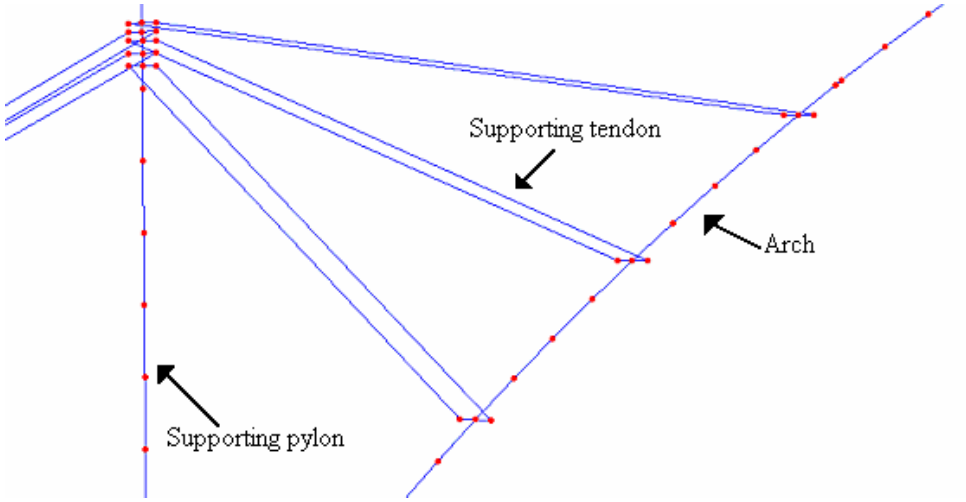

Figure 5.1 Nodes are figured with dots and elements with lines.

In figure 5.2 it can be seen that the model, developed in this thesis, consists of an arch, the superstructure, hangers and piers for the superstructure, two supporting pylons and supporting tendons for the arch. The model also consists of springs at the arch and pier foundations and the tendons are connected to the arch and pylons with auxiliary cross beams, which are too small to be seen in figure 5.2.

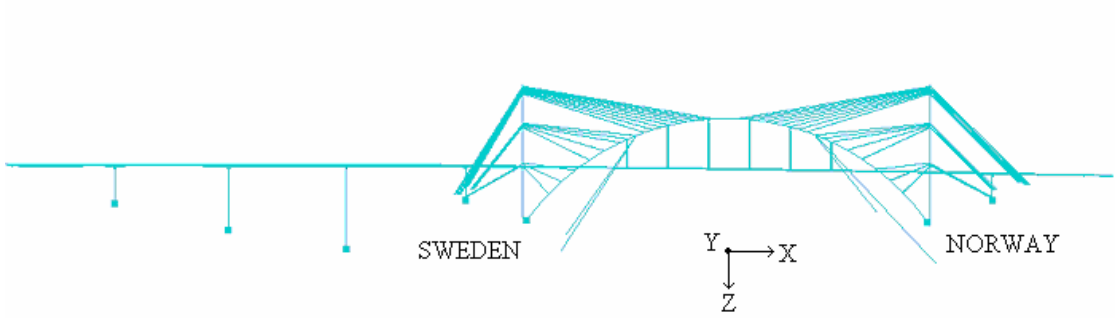

Figure 5.2 The FE-model of the New Svinesund Bridge in ABAQUS, with the completed bridge, the supporting pylons and the supporting tendons.

5.1.2.1 Nodes

The node data is defined in a 3D right-handed, rectangular Cartesian system and contains information of x-, y- and z-coordinates in metres. The coordinate system has a horizontal xy-plane, with a vertical z-axis pointing downwards towards the water. The x-axis is pointing along the arch towards Norway and the y-axis is pointing in transversal direction, in approximately eastern direction, see figure 5.2. The origin is positioned at sea level under the centre of the arch, approximately 90.3 m below the arch crown.

5.1.2.2 Elements

In the model, three different element types, available in ABAQUS, have been used to represent the reality, beam element B31, truss element T3D2 and spring element SPRING1, see Hibbit, Karlsson and Sorensen Inc. (2002).

The concrete arch and the supporting pylons are modelled by the beam elements positioned along their neutral axes. The beam elements have a rectangular, hollow box cross-section, named BOX in ABAQUS. For the BOX section, the height, width and thickness of the section walls are given, see Appendix J for application in ABAQUS.

The hangers that support the carriageways are also modelled with beam elements. However a different cross section, named GENERAL in ABAQUS, is used. Here, the area, the moment of inertia for cross bending and for bending about the first axis and the second axis, the torsional rigidity, the modulus of elasticity, the torsional shear modulus and the coefficient of thermal expansion of the section are defined.

Two nodes truss elements are used for the temporary tendons. To make it possible to vary the amount of strands and the tendon force in a tendon, each tendon was modelled with several parallel truss elements. Each element was modelled as SOLID SECTION. Here the cross sectional area is defined according to Bilfinger Berger (2003).

There are nodes on the sides of the arch and the supporting pylons, where the tendons connect the arch to the supporting pylon and the supporting pylon to the rock anchors. These nodes are coupled to the arch and to the supporting pylons by stiff beam elements. These elements have the same cross section type as the hangers, GENERAL. The stiff beams are only used to help the model to represent the real geometry. Therefore the cross sectional parameters are given fictious values with a very high stiffness and no density.

One-node spring elements are used to model the support stiffness for the piers and the arch, in cases where it is not modelled as fixed or free. For each spring, the degree of freedom is given together with the corresponding linear translational or rotational stiffness, taken from the Bilfinger Berger model (2004).

The piers, supporting the carriageways, are modelled by beam elements positioned along their neutral axes. These elements are also modelled with the cross section GENERAL. Additional stiff beam elements, (with the same properties as the stiff elements in the arch) are used to connect the supports for the carriageways to the pier top.

The carriageways are modelled as beam grid structures to represent their box sections. Each beam in the grid structure was modelled with the cross section GENERAL. For each double-celled box section, three longitudinal beams represent the longitudinal walls with interacting parts of the top and bottom flange. Transversal stiffeners, approximately every fourth meter, represent the internal transversal stiffening walls with interacting parts of the top and bottom flange. At each of the support points, over

the piers and under the hangers from the arch, there are transversal beams connecting the two parallel carriageways. The transversal beams are integrated into each carriageway and are supported between the carriageways. In the model, the transversal beam elements are connected to the carriageway elements and the top nodes of the pier bearings through stiff beam elements. At the end supports, stiff beam elements are also used to connect the carriageway elements to the support nodes. At the connection to the arch, additional stiff beam elements are used to model the interaction that is obtained through the transversal prestressing tendons.

5.1.3 Boundary conditions and constraints

The following assumptions were made regarding the boundary conditions for the bridge:

- The arch was assumed to have a fixed foundation for all degrees of freedom (DOF) except for the rotation around the bridge transverse axis. The support for this DOF was modelled by rotational springs, see Appendix I for application in ABAQUS. The stiffness values were taken from Bilfinger Berger (2002, 2003).

- The piers founded on rock (i.e. piers 2, 3, 5 and 8) were assumed to have a fixed foundation for all translational DOF, and for torsion around the pier axis. The supports for the rotations around the bridge transverse and longitudinal axes were modelled by rotational springs. The stiffnesses according to the indata files of Bilfinger Berger (2004) were used. The stiffnesses for the rotations around the transverse axis correspond to the stiffnesses calculated in Bilfinger Berger (2003). The stiffnesses for the rotations around the longitudinal axis were approximated to be ten times greater.

- The support of pier 4, founded on steel core piles, was modelled by translational and rotational springs for all DOF. The stiffnesses calculated in Bilfinger Berger (2003) were used.

- The temporary pylons were assumed to be fully built-in, with all DOF fixed at the level for their foundation.

- The support at the rock anchors for the temporary tendons was assumed to be completely rigid, with all DOF fixed.

- At the end abutments, on both the Swedish and Norwegian side, each carriageway is supported by two bearings. Here, all support nodes were fixed for displacements in the vertical direction. The support nodes closest to the centre-line of the bridge were fixed also for displacement in the transversal direction. All other DOF were free.

The following assumptions were made regarding the internal connections between the different parts of the structure:

- The carriageways were rigidly connected to the arch, with all degree of freedom equal at the connection.

- The hangers were rigidly connected to the arch as well as to the transversal beams of the carriageways. However, due to the low bending stiffness, the moments transferred through the hangers will be negligible. (The stresses in the hangers, however, may become large due to the bending effect.)

- On the top of the piers, the transversal beams connecting the two carriageways are supported by two bearings. Here, the displacements at the nodes on either side of each bearing were fixed to be equal in the vertical direction. Furthermore, for the eastern of the two bearings on each pier, the displacements in the transversal direction were fixed to be equal. On pier 3 and 4, also the longitudinal displacements were fixed to be equal, for both bearings. All other DOF were free.

The longitudinal and transversal directions used for boundary conditions and internal connections were defined for the current position along the bridge, so that the longitudinal axis points in the tangential direction for the curved part of the bridge.

5.1.4 Material models

The materials used in the FE model, concrete and steel, were modelled as linear elastic. For the concrete in the arch, time dependent properties, i.e. creeping and the development of Young's modulus, have also been taken into account. The concrete in the arch was assumed to be uncracked, although certain cracks were observed during the construction of the bridge. Since the concrete was assumed to be uncracked, the stiffness of the reinforcement steel in concrete was of minor importance and, consequently, the reinforcement was not modelled. In ABAQUS the command *REBAR LAYER, which simplifies the reinforcement modelling, was not possible to use together with beam elements. Another command, *REBAR, could have been used, but was not, due to time limitations and that it was considered to be of minor importance. Using *REBAR, it is needed to model each reinforcement bar in the section separately.

The development of Young's modulus with concrete age, see figure 5.3, was calculated in MATLAB, see Appendix C, according to CEB-FIP Model Code 1990, see Comité Euro-International du Beton (1991), as described in section 3.3. Based on this, indata tables for ABAQUS were calculated in Ms Excel to reflect the concrete maturity in each arch segment separately, based on its casting day. Development of the Young's modulus was only implemented for the concrete belonging to the arch, since it is the structure being analysed. For the supporting pylons an approximation was made for Young's modulus, the value of the 28:th day of maturity was chosen equal to 35.4 GPa. This was done because the casting dates for the pylons were not known exactly and the development of Young's modulus in the pylons is not of great importance in the analysis. The piers were modelled with a value of Young's modulus equal to 33 GPa. This value was taken from the Bilfinger Berger model and was not changed.

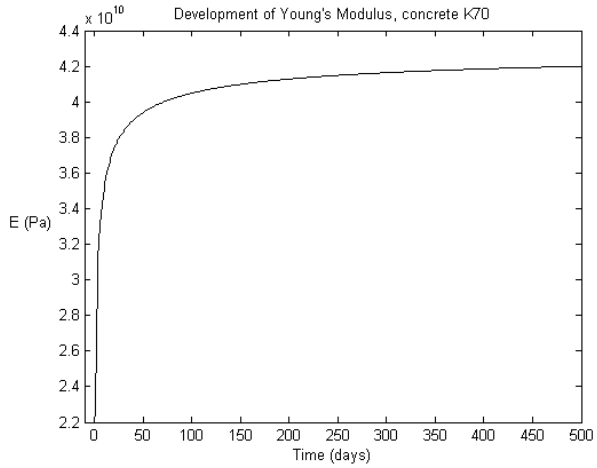

Figure 5.3 The development of Young's modulus in concrete K70 in the arch, according to CEB-FIP Model Code 1990, see Comité Euro-International du Beton (1991).

In order to model the creep and relaxation of concrete in ABAQUS accurately, the material was modelled as viscoelastic in the time domain. For further explanation see section 3.4. For the same reasons as for modelling the Young's modulus, the creep was only modelled for the arch and not for the supporting pylons and piers. See Appendix F for implementation in input file.

In the FE-model, the following elements were modelled as steel: the supporting tendons, the hangers and the elements belonging to the carriageway. The tendons were modelled with the value of Young's modulus equal to 195 GPa. The hangers and the carriageways were modelled with the value of Young's modulus equal to 210 GPa and the density equal to $7.7 \cdot 10^3$ kg/m^3.

5.1.5 Loads

The bridge response was analysed with two different loads taken in account: gravity load and temperature load.

The parts of the bridge that were made of concrete were defined with a density of $2.5 \cdot 10^3$ kg/m^3. This is an approximation made when the reinforcement of the concrete is included. The tendons that were made of steel were approximated to have a density of $7.85 \cdot 10^3$ kg/m^3. The gravity acceleration was approximated to be 10 m/s^2.

The temperature data was taken from SMHI's documentation on the Internet, see www.airviro.smhi.se/svinesund (2004). Tables were generated in Ms Excel and the mean value for each day during construction was calculated. After the construction of the bridge, the analysis continues for another ten years. The temperature in this part of the analysis was only given with one value for each month. These values were taken as the temperature of the first day of each month in the period between October 2003

and September 2004. The temperature data, inserted in ABAQUS input file, are shown in Appendix G.

5.1.6 Modelling of the construction process

When modelling the construction process of the arch, the launching of the arch was subdivided into several stages. Each stage represents one or several construction events happening at the same time. The construction events were divided into three categories. The first category is when an arch segment is constructed. The second category is when a tendon is introduced, modified or removed. The third category is when an arch segment is constructed and a tendon is introduced at the same time. The categories were modelled like this:

- **Category 1: New segment**

  Step 1 – Activating of the elements of a new segment – the step time is equal to one day.

  Step 2 – Loading of the newly activated elements with self-weight – the step time is equal to a very short time period.

  Step 3 – Creep analysis until next event happens – the step time is equal to the period of time between Step 2 and the next construction event.

- **Category 2: Tendon modification**

  Step 1 – Activating and/or deactivating of the elements of a tendon – the step time is equal to a very short time.

  Step 2 – Loading of the newly activated elements with self-weight – the step time is equal to a very short time period.

  Step 3 – Creep analysis until next event happens – the step time is equal to the period of time between Step 2 and the next construction event.

- **Category 3: New segment and tendon modification**

  Step 1 – Activating and/or deactivating of the elements of a tendon – the step time is equal to a very short time.

  Step 2 – Loading of the newly activated elements with self-weight – the step time is equal to a very short time period.

  Step 3 – Activating of the elements of a new segment – the step time is equal to one day.

  Step 4 – Loading of the newly activated elements with self-weight – the step time is equal to a very short time period.

Step 5 – Creep analysis until next event happens – the step time is equal to the period of time between Step 4 and the next construction event.

In the first analysis step, all elements were removed. For the following steps a new part of the model was added or a modification of parameters was made. Creep of concrete was one major priority when modelling the launching. Therefore, the self-weight of the segment was not added until one day after activation, an approximation made in order to obtain more correct creep behaviour of the concrete in this segment. This means that the self-weight of the new segment is applied to the rest of the structure one day after the casting. Even though this is not completely accurate in comparison to reality, the error due to this approximation was considered to be negligible.

For the temporary tendons, the amounts of strands and the tendon force varied. During the launching of the arch, they both increased and decreased, see Appendix E. The tendon forces from Bilfinger Berger (2003) were converted from prestressing jack oil pressure (in bar) to stresses (in MPa) in the strands, trough a calibration relation taken from Bilfinger Berger (2003), see Appendix H. Generally, each tendon was modelled alternatively by different elements; when the prestressing level or the amount of strands were changed, the current element was replaced with a new one with the correct cross-sectional area and the new prestress level as initial stress. Each time a modification of a tendon was done, it was modelled as a construction event of category 2. In the first step in the sequence, the no longer accurate element set was deactivated and the new correct element set was activated, see Appendix F.

When the launching of the arch was completed, the temporary supporting structure was removed. At last the permanent piers, hangers and carriageways are added to the arch.

6 Analysis results

In the analysis, three different kinds of results were considered to be of special interest. These were the deformations of the arch during the launching, the strain variations in the points where strain gauges were located and sectional forces and moments within the arch after completion. Other results have also been observed such as stresses within the arch and temporary cables and the temperature variation in the structure.

When analysing the whole bridge with viscoelastic material properties in the concrete of the arch, the FE analysis becomes far more complicated and the computational time required in order to complete the analysis is much greater than if viscoelasticity is not included or if the permanent piers, hangers and carriageways are not added to the model. The computational time required was so immense that with the computer capacity available, results could not be obtained from the FE analysis. Therefore, the results presented and discussed in this chapter are for different FE models of the arch and temporary supporting structure only. Four different models were compared to each other to see the effects of different phenomena that were included in the models, see Table 6.1 for the differences of the models.

Table 6.1 Table showing what the four models included. In Model 4 the completed arch was assembled in one step.

	Model			
Included in the model	1	2	3	4
Stepwise launching of the arch	X	X	X	
Viscoelastic creep	X	X		
Development of Young's modulus	X	X		
Temperature variations	X			

6.1 Deformations

The deformations in the arch during launching are of interest to examine as they can be compared with measurements or calculations made by Bilfinger Berger. However, when new elements were added to the model during the launching of the arch, the new nodes in the new elements were added in their original position, even though the previously added elements had already deformed. This means that the new element closest to a previously added element will obtain an incorrect orientation and the deformed shape of the arch looks quite strange and unrealistic, see figure 6.1.

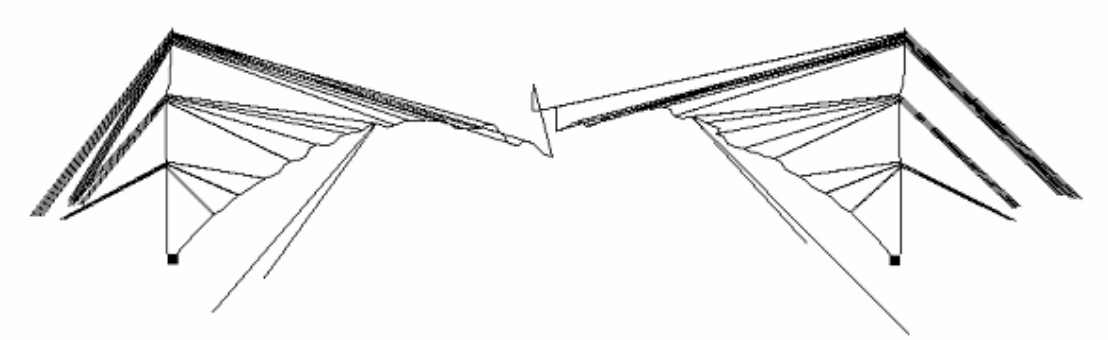

Figure 6.1 Deformed shape of the arch after completion, obtained from Model 3. The deformation scale factor is 50. The supporting pylons and cables are visible in the figure although they have been removed.

The deformed shape of the arch obtains a wavy character because new elements added closest to a previously added element obtain an incorrect orientation; this is due to the fact that already active elements have deformed due to self-weight and the force in the prestressing cables. Depending on if a new element is added after a previous element has been loaded with self-weight or after a cable has been activated and prestressed is of importance for the deformed shape of the new element.

If a comparison is made between Model 3 and Model 4 it is clearly visible that the modelling of the launching procedure affects the results concerning deformations, see figure 6.2.

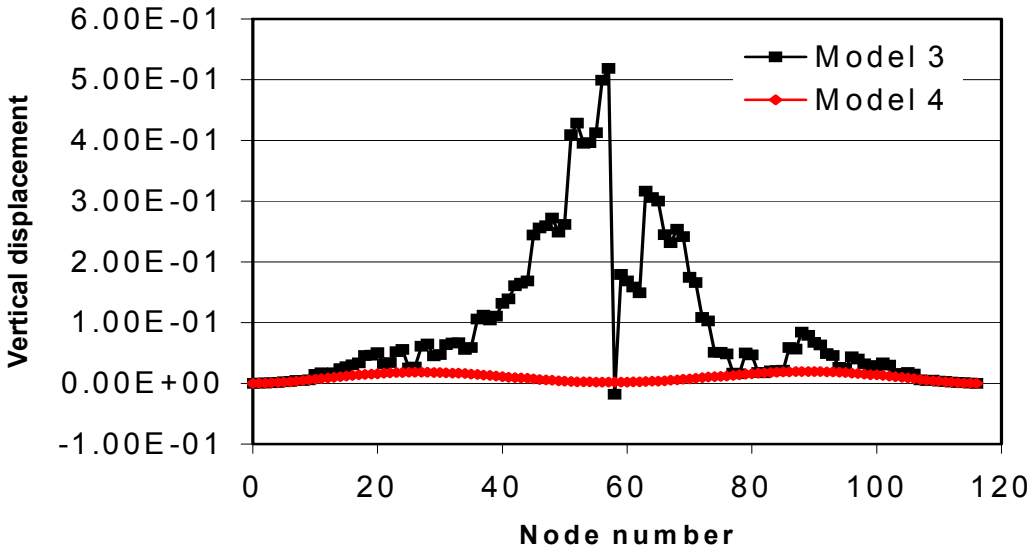

Figure 6.2 Vertical displacements in the nodes for Model 3 and Model 4.

It can be seen in figure 6.2 that the deformations in Model 3 far exceed the deformations in Model 4. The maximum vertical displacement in Model 3 is over half a metre. It can also be seen that the vertical displacements in Model 3 vary extensively from node to node. The deformations obtained in Model 3 represents the

deformations from the casting position to the final position for the arch segments, deformations that were actively controlled by the contractor during construction. One possibility could be to compare the deformations from the analysis with the position measurements of the arch, continuously made by the contractor. However, this is a quite extensive work and had to be left out of this thesis.

6.2 Sectional forces and moments

The arch was assumed to have a fixed foundation for all degrees of freedom (DOF) except for the rotation around the bridge transverse axis. The support for this DOF was modelled by rotational springs at each foundation. The stiffness value for these two springs is however so high that the sectional moments close to the abutments become large, see figure 6.3. The moment distribution along the arch for the different models is also within the range that could be expected. The shear force distribution for the different models can be seen in figure 6.4 and also the shear force distribution looks reasonable. Considering the normal force distribution it can be seen in figure 6.5 that the whole arch is under compression. This was expected because the main structural behaviour of arch structures is to carry the load through compression in the arch.

When comparing the different sectional forces and moments for the different FE models some differences in the results could be seen. The differences between the FE models affected the results to very different extent, see figures 6.3-6.5. It can be seen in the figures that Model 4 is the FE model whose results differ the most compared with the other models. Whereas the sectional forces and moments obtained from Model 1, Model 2 and Model 3 coincide very much. Consequently, it can be said that including the construction process in the modelling has a great influence on the results. In contrary, modelling of the development of Young's modulus, creep and temperature effect does not affect the results in terms of sectional forces and moments remarkably much. The temperature differences between the activation of the different segments and the end of analysis vary widely, see figure 6.7. Therefore it is complicated to evaluate why the temperature variations did not affect the results.

When comparing the sectional moments between Model 3 and Model 4 in figure 6.3 it can be seen that the effect of including the construction process in the modelling is that the sectional moment becomes higher (i.e. more positive) throughout the arch. This means that the moments at the abutments become larger for Model 3 than for model 4. This is where the largest moment in the whole arch appears and it is also where the difference between the two models is most pronounced. Another observation that can be made is that the moment becomes negative within certain regions for Model 4 whereas, for the other models, the negative moment is negligible.

In figure 6.4 and figure 6.5 it can be seen that the differences in sectional shear force and normal force between the different models are not that remarkable, but also here it is Model 4 that has slightly different results compared to the other models. The difference between the shear force distribution in Model 4 and the other models is that, for Model 4, the absolute value of the shear force near the abutments is lower and, between the points were the shear force changes sign, the absolute value is higher. These points are approximately 50 metres from the abutments. The difference

in normal force is even smaller but it can be seen that Model 4 has slightly lower normal force in the mid part of the arch, compared to the other models.

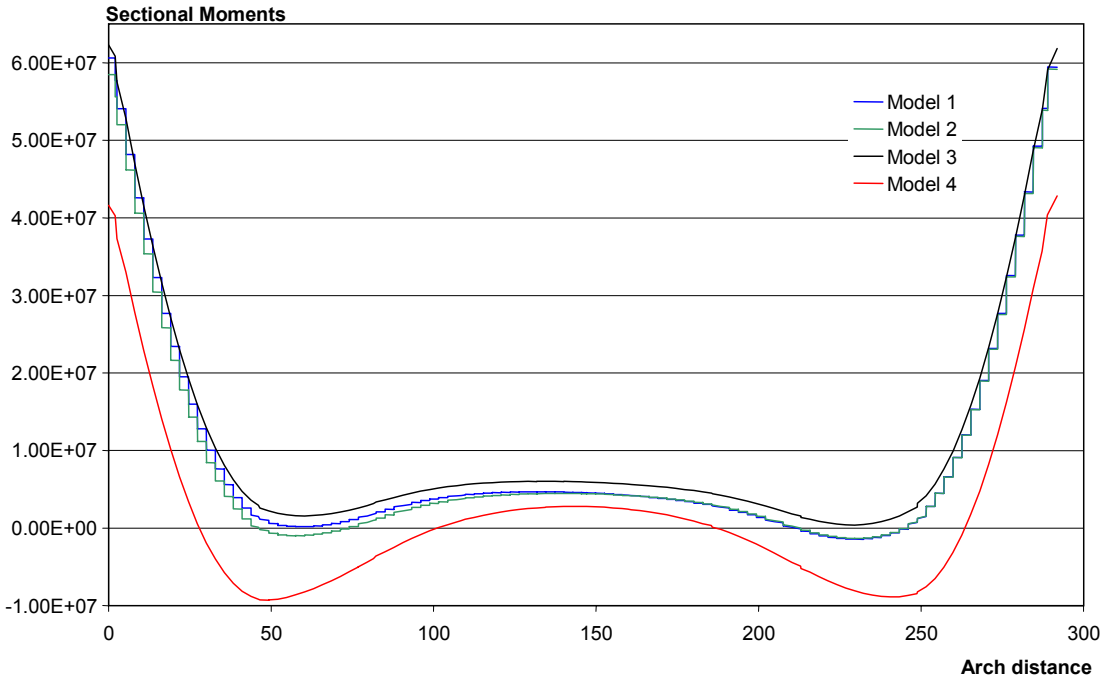

Figure 6.3 *Sectional Moments for the arch subjected to gravity for the different FE models.*

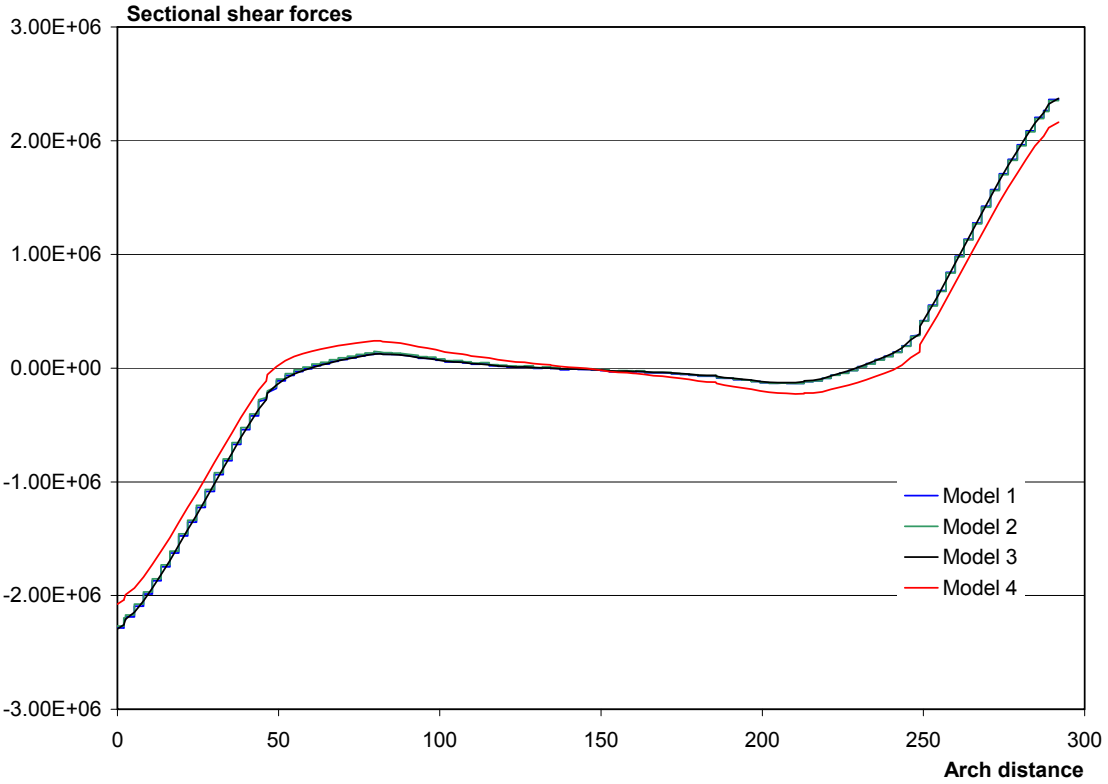

Figure 6.4 *Sectional Shear forces for the arch subjected to gravity for the different FE models.*

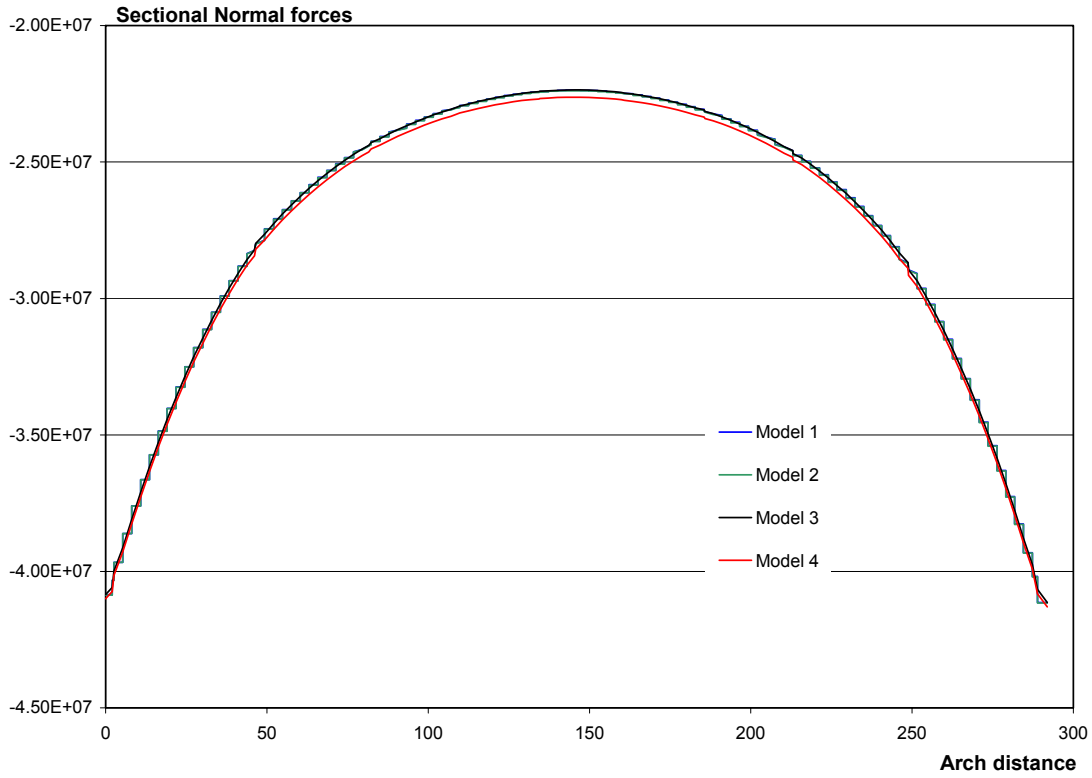

Figure 6.5 Sectional Normal forces for the arch subjected to gravity for the different FE models.

In figures 6.3-6.5 it can be seen that the results from Model 1 and Model 2 have a jagged appearance. This is believed to be due to the fact that these two models have variations in stiffness (Young's modulus) along the arch.

6.3 Strains and temperature

The strain variations in certain cross-sections of the arch are of specific interest as they can be compared with the field measurements performed on the bridge and thereby the modelling of the sequential construction can be evaluated. Results from the following strain gauges were obtained from the monitoring project: **VWS1-T**, **VWS1-B**, **VWS6-T**, **VWS6-B**, **RSS25-T** and **RSS25-B (**for labelling of the gauges, see section 4.3.2**)**. The results from the two sensors in segment 25 are not compared with the FE results since the launching of the carriageways was not successful in the FE analysis and, consequently, the strain variations obtained in the analysis for segment 25 cannot be compared with the measurements. For the other four sensors, the measurements can be compared with the analysis results until the launching of the carriageways was performed.

In the figures 6.6, 6.8, 6.10 and 6.12 the strain variations from Model 1 and Model 2 can be seen compared with their respective results from the strain gauges in the same position and in the figures 6.7, 6.9, 6.11 and 6.13 the temperature variation in Model 1

is compared with the real temperature variations measured in the different positions of the arch.

Strain values can only be obtained in the integration points in ABAQUS and these points do not coincide exactly with the position of the strain gauges. The strain gauges are situated in the outer main reinforcement layer, assumed to be 15 cm from the outer edge of the cross-section. In order to be able to compare the results, the values of the strains from the FE analysis were linearly interpolated to the position of the gauge.

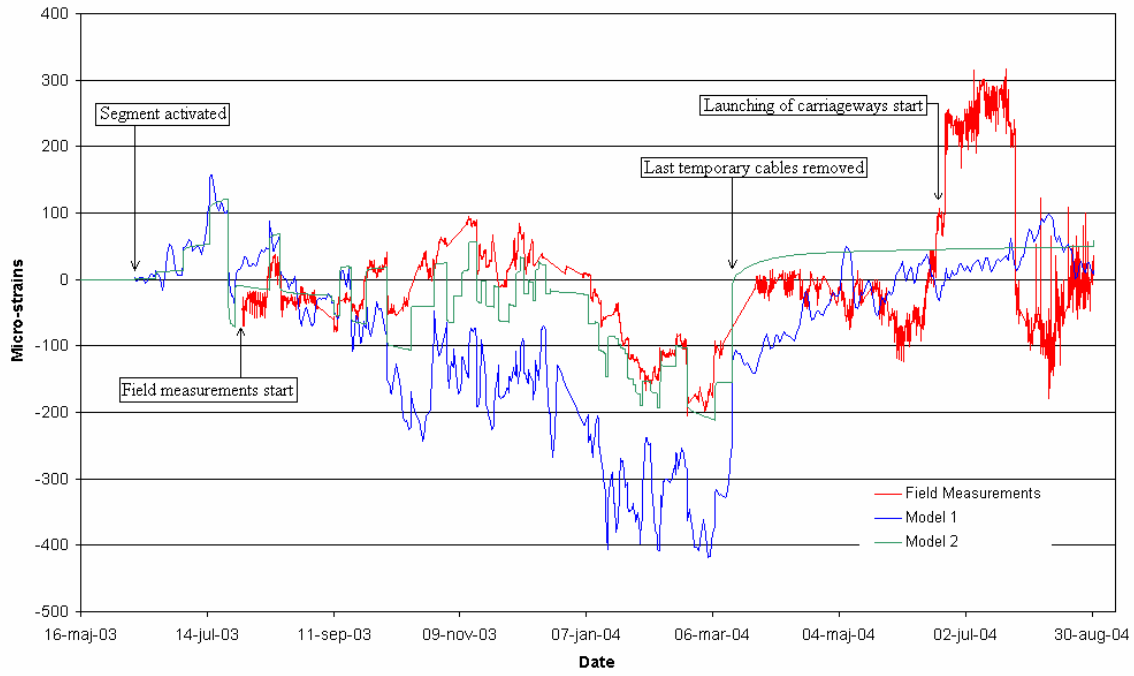

*Figure 6.6 Strains obtained from FE analyses and field measurements at gauge position **VWS1-T** in the top of segment 1 on the Swedish side.*

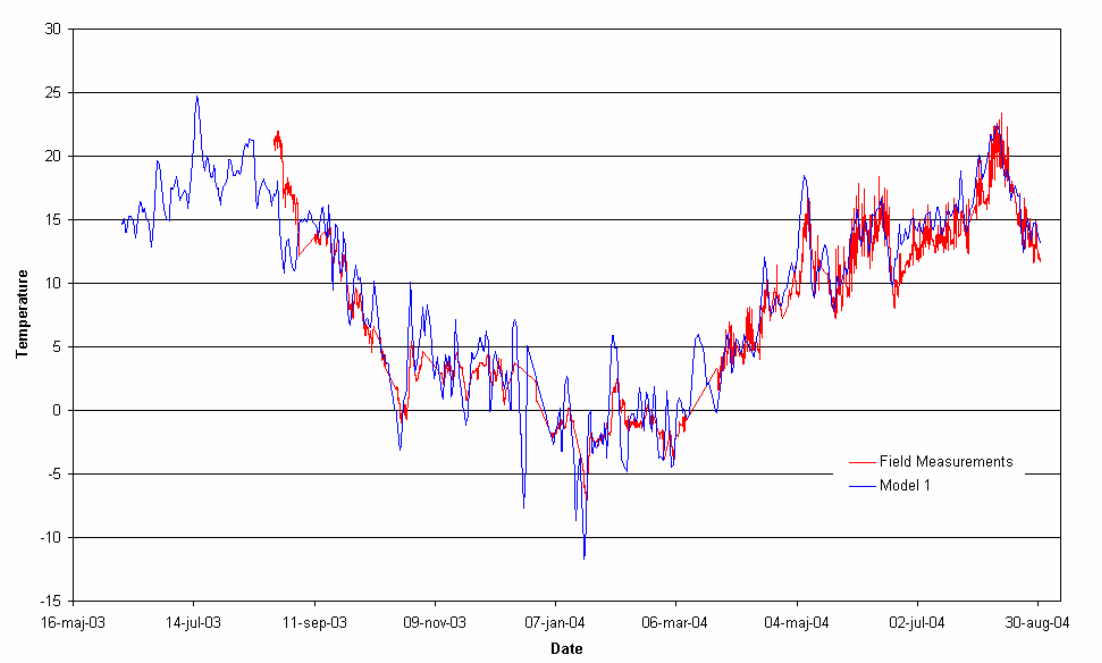

Figure 6.7 *Temperature obtained from FE analyses, compared to the temperature measured at gauge position **VWS1-T** in the top of segment 1 on the Swedish side.*

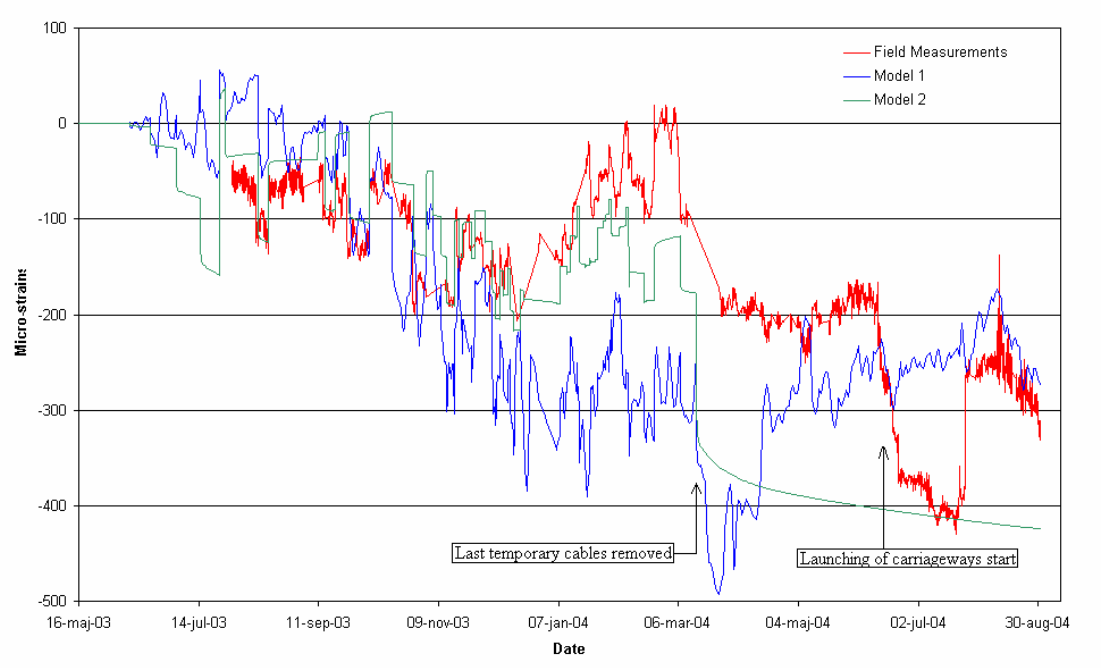

Figure 6.8 *Strains obtained from FE analyses and field measurements at gauge position **VWS1-B** in the bottom of segment 1 on the Swedish side.*

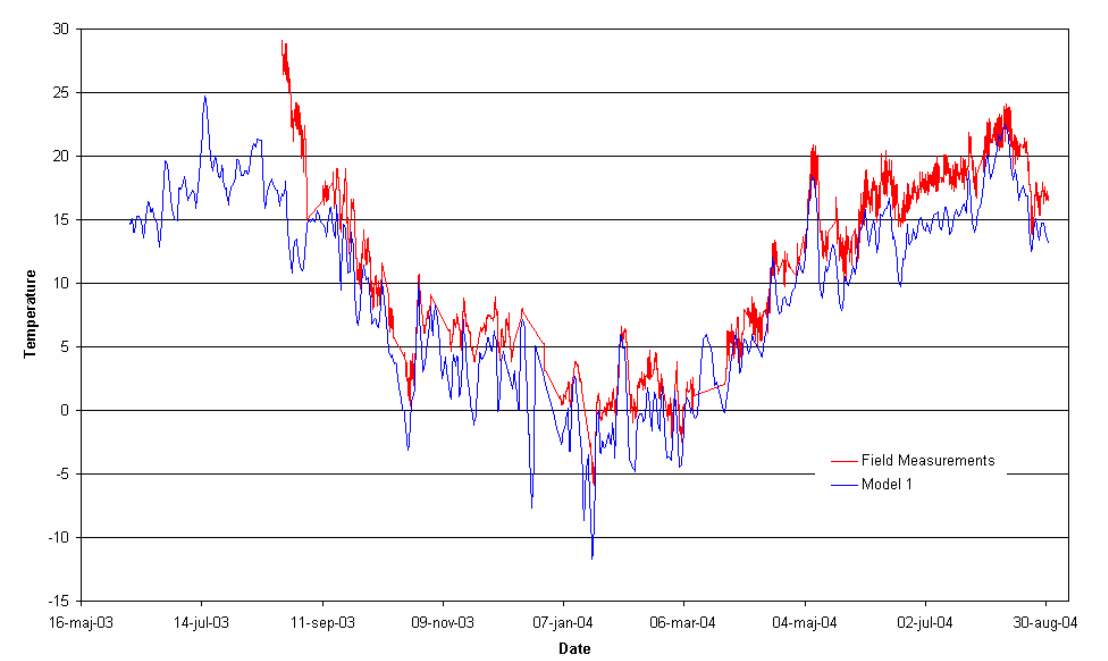

Figure 6.9 *Temperature obtained from FE analyses, compared to the temperature measured at gauge position **VWS1-B** in the bottom of segment 1 on the Swedish side.*

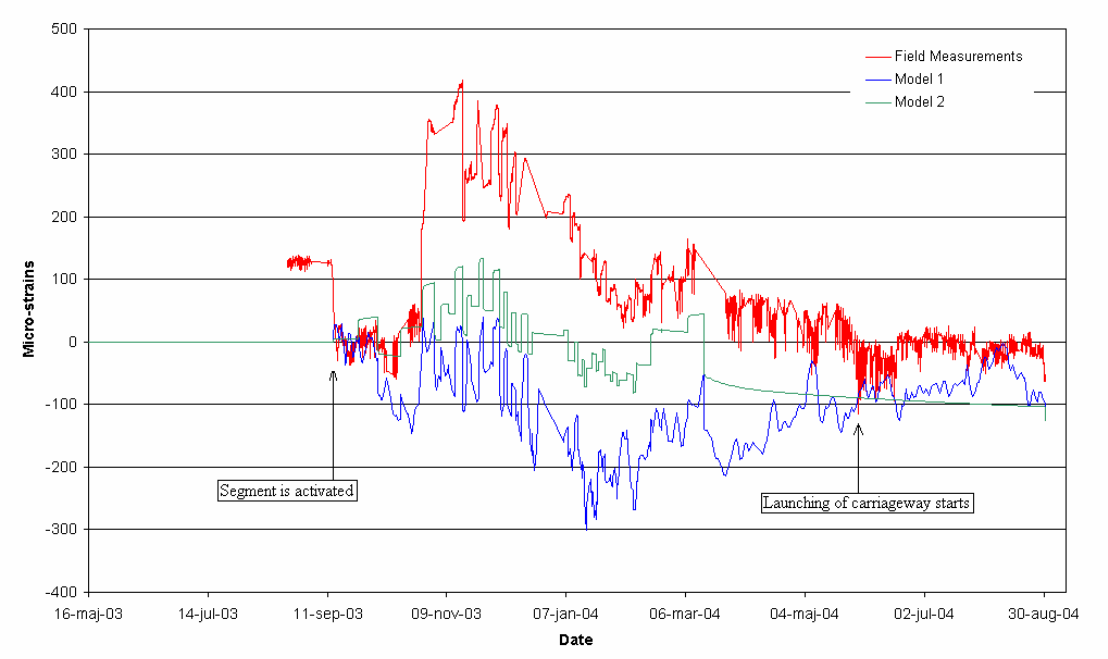

Figure 6.10 *Strains obtained from FE analyses and field measurements at gauge position**VWS6-T** in the top of segment 6 on the Swedish side.*

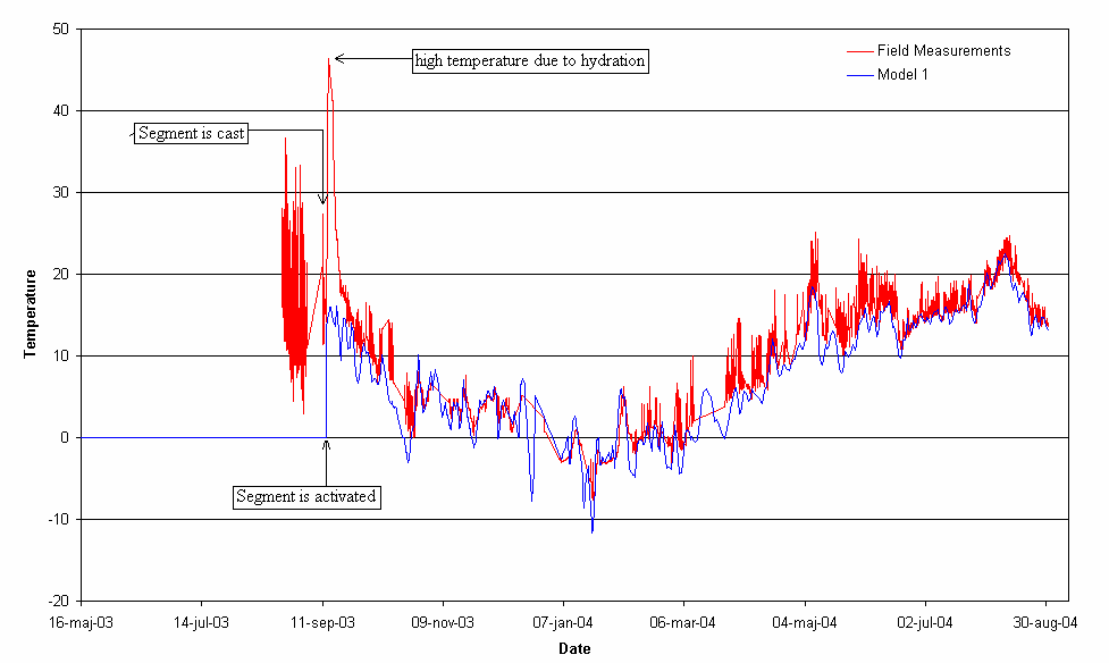

*Figure 6.11 Temperature obtained from FE analyses, compared to the temperature measured at gauge position **VWS6-T** in the top of segment 6 on the Swedish side.*

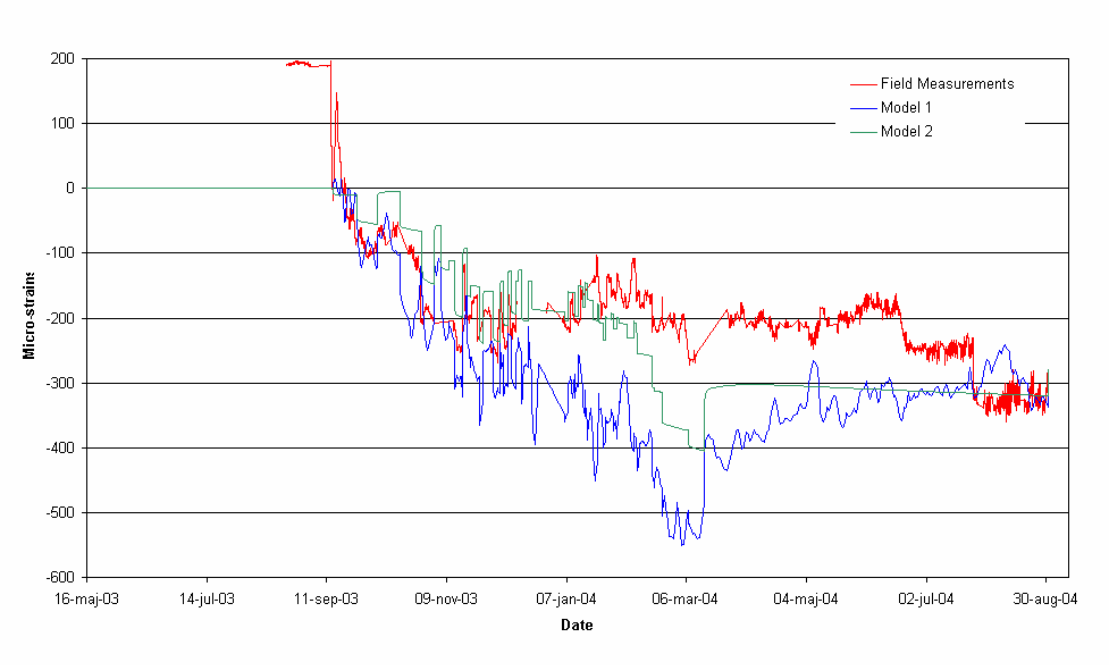

*Figure 6.12 Strains obtained from FE analyses and field measurements at gauge position**VWS6-B** in the bottom of segment 6 on the Swedish side.*

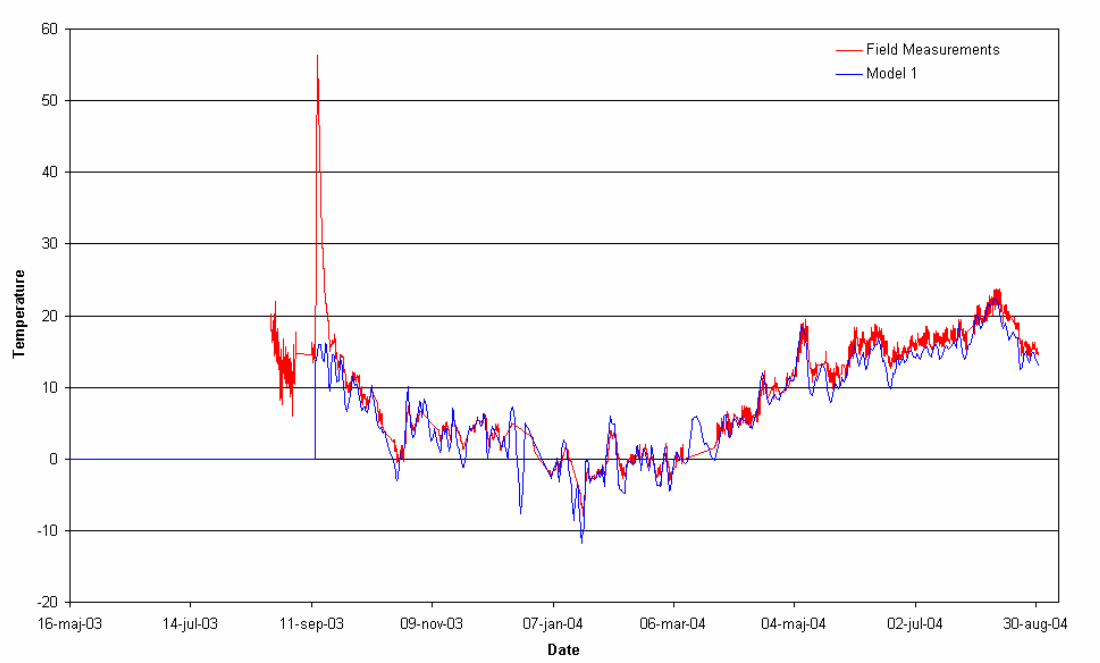

*Figure 6.13 Temperature obtained from FE analyses, compared to the temperature measured at gauge position **VWS6-B** in the bottom of segment 6 on the Swedish side.*

In order to understand the strains diagrams better, some aspects will be pointed out. The only difference between Model 1 and Model 2 is that Model 1 is subjected to temperature load. This can clearly be seen in all diagrams; the strains in Model 1 vary continuously due to temperatures variations. However, in Model 2, the only changes of strain in between the different construction events are due to creep. This can be seen for example in figure 6.6, where a typical creep curve is visible after the last temporary cables have been removed.

The different construction events in the modelling are casting of segments and modifications of tendons, as explained in chapter 5.1.6. Casting a new segment, removing tendons and decreasing the force in tendons all cause the arch to deform downwards and consequently also adds extra tension to the top of the segments while it adds more compression to the bottom of the segments. One very apparent example of this can be seen in figure 6.6 and 6.8 when the last temporary cables are removed (except for the transverse cables). The opposite happens when new tendons are installed and when the force in existing tendons is increased.

When the strains obtained from the field measurements are examined it can be seen that the measurements from segment 1 are only recorded from the 30:th of July and forward although the segment was actually cast prior to this. The temperature measurements for segment 1 are recorded from the 22:nd of August and forward. In figures 6.10-6.13 it can be seen that both data for the strains as for temperature has been recorded before the date of casting for segment 6. The information obtained from the sensors before the date of casting which was on the 19:th of September should be neglected. In all the figures, from figure 6.6 to figure 6.13, it can also be seen that there have been interruptions in the recording of data. This can be seen when there is a straight line from one date to another.

The strains obtained from field measurements have obviously been influenced to a great extent by the launching of the carriageways. For segment 1 this can be seen very clearly in figure 6.6 and 6.8 whereas for segment 6 the launching of the carriageways is not so obvious, see figure 6.10 and 6.12.

When comparing the temperatures used in FE analysis with the actual temperatures in the different points inside the arch, it can be seen in the figures (6.7, 6.9, 6.11 and 6.13) that the temperature has been modelled in a reasonable way. The main difference between the temperature used in the FE modelling and the real temperature in the concrete is that the heating effect of hydration could not be modelled, see figure 6.11 and 6.13. Also, the temperature variation inside the concrete seems to be smaller than the variation of the daily mean value of the air temperature.

From the strain diagrams it can be seen that the modelling of the sequential construction does not coincide exactly with the results obtained from the field measurements. There can be many reasons for this, partly discussed in section 2. One interesting remark that can be made is that Model 2 seems to agree better with field measurements than Model 1, although the modelling of the temperature variation seemed to be reasonable. On the other hand the variation of temperature did not influence the sectional forces and moments, which was seen in figures 6.3-6.5.

7 Conclusions

In this thesis the following was achieved:

- A finite element model of the New Svinesund Bridge has been further developed and a more accurate analysis of the launching of the arch has been made based on the real launching procedure, registered by the contractor.

- Material models for creep of concrete have been evaluated and the concrete in the arch has been modelled with a viscoelastic material model. This material model cannot be combined with non-linear material models, e.g. for cracking, due to limitations in the FE program used, ABAQUS.

- The analysis of the launching of the arch also included the development over time of the Young's modulus in the concrete and the temperature variations over time.

- The results from the analysis have been compared with field measurements and with a simplified analysis without the modelling of the launching of the arch.

The following conclusions can be drawn based on the results obtained from the FE analysis:

- The deformations obtained during launching of the arch were much greater than the deformations that occur for the completed arch. However, these results were too complicated to evaluate and to compare to measurements and the evaluation had to be omitted.

- The stepwise launching of the arch had large effect on the sectional forces and moments, especially the bending moments. The sectional moments near the abutments increased with approximately 50% when the arch was subjected to gravity. It could not be shown that the viscoelastic creep, development of Young's modulus or temperature variations affected the sectional forces and moments.

- The strains in the arch during the construction can be observed in the analysis and the different construction events can clearly be seen when the strain diagrams are interpreted. The temperature variations affect the strains extensively, both in reality and in the analysis. Therefore it is extremely difficult to evaluate the modelling of the launching of the arch. One way to evaluate the accuracy of the modelling could be through studying specific construction events, which occur during short time periods. However, this could not be included in this thesis.

When analysing the whole bridge structure with viscoelastic material properties in the arch, the computational time needed to complete the analysis became very long and the analyses were aborted due to exceeding the accessible time limit. It is recommended that it is further investigated if it is possible to reduce the computational time by making the FE model and analysis more efficient.

Other possible improvements to the FE analysis of the arch launching are the following:

- Modelling of nodes in original casting position. The node positions may then be compared to the position of the arch segments, continuously measured during launching.

- To include shrinkage and cracking of the concrete. However, this requires further development of the material models, compared to what is available in ABAQUS today.

- Studying the modelling of temperature effect in detail and to model the temperatures in the arch according to the temperature measurements made in the arch.

Improvements can also be made to the evaluation:

- The analysis deformations can be compared with measurements made of the change of positions during launching.

- The effect of specific events during construction can be studied, such as stress regulations, addition of loads (carriageways) and sudden temperature changes.

- The dynamic properties can be compared with measured mode data, such as eigenmodes and eigenfrequencies, for different stages in the launching.

When a FE model of an actual structure is developed in order to be used for strength assessment it is of great importance that all relevant information is stored and that it is available for the developers of the model. In this case study of the New Svinesund Bridge, all information was not available for the modelling of the bridge. Consequently, it was necessary to make reasonable assumptions and approximations. Even if all information could be available for the structural assessment the real structural behaviour cannot be modelled perfectly due to limitations in the available methods of modelling. Consequently, it is of importance to make good choices in the way of modelling the structure.

8 References

AB Svensk Byggtjänst (1994): *Betonghandbok, Material*, Svenskt Tryck AB, Stockholm, Sweden, 1127 pp.

Bilfinger Berger (2003): *K Comparative Analysis of Global System for Design of Substructure and L Launching of the arch*, Bilfinger Berger AG (Document no. 110K1301 rev A1, 110K1302 rev B2, 110K1303 rev A, 116K1301 rev A1, 116K1303 rev 0, 116K1305 rev 0, 116K1321 rev A), Mannheim, Germany.

Bilfinger Berger (2004): *Indata files for the structural model of the New Svinesund Bridge*, Text files obtained by e-mail from Bilfinger Berger AG, Mannheim, Germany.

Boverket (1994): *Boverkets handbok om betongkonstruktioner, Band 1, Konstruktion,* AB Svensk Byggtjänst, Stockholm, Sweden

Cederwall, K. (2000): *Time dependent behavior due to creep and shrinkage in concrete*, Compendium 96:10, Department of Structural Engineering, Concrete Structures, Gothenburg, Sweden.

Comité Euro-International du Beton (1991): *CEB-FIP Model Code 1990*, Comité Euro-International du Beton, Lausanne, Switzerland.

CEN (2002): Eurocode 2: *Design of concrete structures – Part 1: General rules and rules for buildings*, European standard, Brussels.

COST 345 (2001): *Procedures Required for Assessing Highway Structures*, Working Group WG 4 and WG 5 Report, Luxembourg: Office for Official Publications of the European Communities, Luxemburg, Belgium.

Engström, B. (1999): *Beräkning av betong- och murverkskonstruktioner – Del 1 – Grunder*, Institutionen för konstruktionsteknik, Betongbyggnad, Gothenburg, Sweden.

FB Centrallaboratorium (2004): *Provning av hårdnad betong*, Files obtained from Bilfinger Berger.

Ghali, A., Favre, R. (1994): *Concrete Structures: Stresses and Deformations – Second Edition*, E & FN Spon, London, UK.

Hibbit, Karlson and Sorensen Inc. (2002): *Abaqus/Standard Version 6.3, User's Manual, Theory Manual and Keywords Manual*, Hibbit, Karlson, and Soresen Inc., U.S.A..

James, G., Karoumi, R. (2003): *Monitoring of the New Svinesund Bridge – Report 1: Instrumentation of the arch and preliminary results from the construction phase*, Department of Civil and Architectural Engineering, KTH, Stockholm, Sweden.

Plos, M., Gylltoft, K. (2002): *Bärighetsutredningar av broar i framtiden - Nyanserade beräkningsmetoder såsom finit elementmetod*, report 02:6, Department of Structural Engineering, Chalmers University of Technology, Gothenburg, Sweden.

Plos, M., Movaffaghi, H. (2004): *Finite Element Analysis of the New Svinesund Bridge – Design model conversion and analysis of the arch launching*, report 04:12, Department of Structural Engineering and Mechanics, Concrete Structures, Chalmers University of Technology, Gothenburg, Sweden.

Sofistik (2001): *Sofistik manuals: AQUA Version 11.40, GENF Version 10.20 and STAR2 Version 10.20*, Sofistik AG, Oberschleissheim, Germany

www.airviro.smhi.se/svinesund (2004).

www.vv.se/svinesundsforbindelsen (uppdaterad 2004-11-23).

Appendix A. ABAQUS input file for material properties for concrete in the arch.

In the text below the material definition for the Swedish abutment SS0 is shown only. The rest of the arch is defined in the same way.

```
****************** MATERIAL PROPERTIES FOR CONCRETE IN THE ARCH**************
**
**                     E = YOUNG'S MODULUS
**                    NU = POISSON'S RATIO
**                    FV = FIELD VARIABLE
**                  GR(T)= DIMENSIONLESS SHEAR RELAXATION MODULUS
**                  KR(T)= DIMENSIONLESS BULK RELAXATION MODULUS
**                     T = TIME
**
**  MATERIAL DEFENITION FOR THE ABUTMENT ON THE SWEDISH SIDE
*MATERIAL, NAME=SS 0
*ELASTIC, MODULI=INSTANTANEOUS, DEPENDENCIES=1
**     E           ,     NU    ,     FV
       22325421267 ,     0,2   ,     1
       37897163157 ,     0,2   ,     2
       37994643668 ,     0,2   ,     3
       38618373958 ,     0,2   ,     4
       38681460377 ,     0,2   ,     5
       38741996253 ,     0,2   ,     6
       39318435168 ,     0,2   ,     7
       39356954979 ,     0,2   ,     8
       39716732312 ,     0,2   ,     9
       39744655863 ,     0,2   ,     10
       39946300591 ,     0,2   ,     11
       39969109074 ,     0,2   ,     12
       40013329198 ,     0,2   ,     13
       40034772218 ,     0,2   ,     14
       40192110982 ,     0,2   ,     15
       40210181528 ,     0,2   ,     16
       40312206534 ,     0,2   ,     17
       40328223329 ,     0,2   ,     18
       40343978636 ,     0,2   ,     19
       40359479525 ,     0,2   ,     20
       40404522479 ,     0,2   ,     21
       40461403254 ,     0,2   ,     22
       40488583332 ,     0,2   ,     23
       40501876256 ,     0,2   ,     24
       40540623019 ,     0,2   ,     25
       40601685087 ,     0,2   ,     26
       40613405698 ,     0,2   ,     27
       40691282296 ,     0,2   ,     28
       40701849617 ,     0,2   ,     29
       40712286148 ,     0,2   ,     30
       40732777507 ,     0,2   ,     31
       40742837481 ,     0,2   ,     32
       40781896064 ,     0,2   ,     33
       40791376872 ,     0,2   ,     34
       40800748525 ,     0,2   ,     35
       40846040574 ,     0,2   ,     36
       40854799230 ,     0,2   ,     37
```

40863462233 , 0,2 , 38
40937397318 , 0,2 , 39
40945192425 , 0,2 , 40
41004825099 , 0,2 , 41
41011956454 , 0,2 , 42
41019019907 , 0,2 , 43
41046615830 , 0,2 , 44
41053355423 , 0,2 , 45
41086144959 , 0,2 , 46
41092527501 , 0,2 , 47
41129666039 , 0,2 , 48
41135670369 , 0,2 , 49
41141623728 , 0,2 , 50
41147526835 , 0,2 , 51
41170650652 , 0,2 , 52
41176312811 , 0,2 , 53
41181928750 , 0,2 , 54
41187499096 , 0,2 , 55
41198505462 , 0,2 , 56
41203942678 , 0,2 , 57
41209336696 , 0,2 , 58
41214688085 , 0,2 , 59
41219997407 , 0,2 , 60
41225265211 , 0,2 , 61
41230492037 , 0,2 , 62
41235678417 , 0,2 , 63
41245931906 , 0,2 , 64
41251000029 , 0,2 , 65
41261021501 , 0,2 , 66
41265975809 , 0,2 , 67
41270893125 , 0,2 , 68
41280618610 , 0,2 , 69
41285427675 , 0,2 , 70
41290201539 , 0,2 , 71
41294940630 , 0,2 , 72
41299645370 , 0,2 , 73
41304316174 , 0,2 , 74
41308953447 , 0,2 , 75
41318129001 , 0,2 , 76
41322668061 , 0,2 , 77
41327175155 , 0,2 , 78
41336094933 , 0,2 , 79
41340508348 , 0,2 , 80
41344891257 , 0,2 , 81
41349244013 , 0,2 , 82
41353566959 , 0,2 , 83
41357860436 , 0,2 , 84
41362124778 , 0,2 , 85
41366360314 , 0,2 , 86
41370567368 , 0,2 , 87
41434252294 , 0,2 , 88
41441764547 , 0,2 , 89
41445485768 , 0,2 , 90
41449184037 , 0,2 , 91
41452859591 , 0,2 , 92
41460143480 , 0,2 , 93
41463752268 , 0,2 , 94
41467339251 , 0,2 , 95
41470904646 , 0,2 , 96
41474448672 , 0,2 , 97

```
      41481473461 ,     0,2   ,     98
      41484954643 ,     0,2   ,     99
      41488415290 ,     0,2   ,     100
      41491855603 ,     0,2   ,     101
      41495275781 ,     0,2   ,     102
      41498676022 ,     0,2   ,     103
      41502056517 ,     0,2   ,     104
      41505417458 ,     0,2   ,     105
      41508759034 ,     0,2   ,     106
      41515384828 ,     0,2   ,     107
      41518669411 ,     0,2   ,     108
      41521935357 ,     0,2   ,     109
      41525182841 ,     0,2   ,     110
      41528412038 ,     0,2   ,     111
      41534816252 ,     0,2   ,     112
      41537991605 ,     0,2   ,     113
      41541149344 ,     0,2   ,     114
      41544289630 ,     0,2   ,     115
      41547412624 ,     0,2   ,     116
      41550518485 ,     0,2   ,     117
      41553607370 ,     0,2   ,     118
      41556679432 ,     0,2   ,     119
      41559734824 ,     0,2   ,     120
      41562773698 ,     0,2   ,     121
      41568802480 ,     0,2   ,     122
      41571792681 ,     0,2   ,     123
      41574766946 ,     0,2   ,     124
      41577725417 ,     0,2   ,     125
      41580668235 ,     0,2   ,     126
      41589404131 ,     0,2   ,     127
      41592285693 ,     0,2   ,     128
      41628428387 ,     0,2   ,     129
      41649526678 ,     0,2   ,     130
      41911451798 ,     0,2   ,     131
      41962777633 ,     0,2   ,     132
      42813950792 ,     0,2   ,     133
**
*DENSITY
      2,50E+03
*EXPANSION, TYPE=ISO
      1,00E-05
**
**
*VISCOELASTIC, TIME=RELAXATION TEST DATA
**
*COMBINED TEST DATA
**   GR(T)  ,          KR(T)  ,      T
    0.9175  ,         0.9175  ,     0.1
    0.9003  ,         0.9003  ,     0.2
    0.8888  ,         0.8888  ,     0.3
    0.8800  ,         0.8800  ,     0.4
    0.8728  ,         0.8728  ,     0.5
    0.8666  ,         0.8666  ,     0.6
    0.8612  ,         0.8612  ,     0.7
    0.8563  ,         0.8563  ,     0.8
    0.8519  ,         0.8519  ,     0.9
    0.8479  ,         0.8479  ,     1
    0.8441  ,         0.8441  ,     1.1
    0.8407  ,         0.8407  ,     1.2
    0.8374  ,         0.8374  ,     1.3
```

0.8344	0.8344	1.4
0.8315	0.8315	1.5
0.8288	0.8288	1.6
0.8262	0.8262	1.7
0.8237	0.8237	1.8
0.8214	0.8214	1.9
0.8191	0.8191	2
0.8169	0.8169	2.1
0.8148	0.8148	2.2
0.8128	0.8128	2.3
0.8109	0.8109	2.4
0.8090	0.8090	2.5
0.8072	0.8072	2.6
0.8054	0.8054	2.7
0.8037	0.8037	2.8
0.8020	0.8020	2.9
0.8004	0.8004	3
0.7988	0.7988	3.1
0.7973	0.7973	3.2
0.7958	0.7958	3.3
0.7944	0.7944	3.4
0.7929	0.7929	3.5
0.7915	0.7915	3.6
0.7902	0.7902	3.7
0.7889	0.7889	3.8
0.7876	0.7876	3.9
0.7863	0.7863	4
0.7850	0.7850	4.1
0.7838	0.7838	4.2
0.7826	0.7826	4.3
0.7815	0.7815	4.4
0.7803	0.7803	4.5
0.7792	0.7792	4.6
0.7781	0.7781	4.7
0.7770	0.7770	4.8
0.7759	0.7759	4.9
0.7749	0.7749	5
0.7738	0.7738	5.1
0.7728	0.7728	5.2
0.7718	0.7718	5.3
0.7708	0.7708	5.4
0.7699	0.7699	5.5
0.7689	0.7689	5.6
0.7680	0.7680	5.7
0.7670	0.7670	5.8
0.7661	0.7661	5.9
0.7652	0.7652	6
0.7643	0.7643	6.1
0.7635	0.7635	6.2
0.7626	0.7626	6.3
0.7617	0.7617	6.4
0.7609	0.7609	6.5
0.7601	0.7601	6.6
0.7592	0.7592	6.7
0.7584	0.7584	6.8
0.7576	0.7576	6.9
0.7568	0.7568	7
0.7561	0.7561	7.1
0.7553	0.7553	7.2
0.7545	0.7545	7.3

0.7538	0.7538	7.4
0.7530	0.7530	7.5
0.7523	0.7523	7.6
0.7516	0.7516	7.7
0.7508	0.7508	7.8
0.7501	0.7501	7.9
0.7494	0.7494	8
0.7487	0.7487	8.1
0.7480	0.7480	8.2
0.7474	0.7474	8.3
0.7467	0.7467	8.4
0.7460	0.7460	8.5
0.7454	0.7454	8.6
0.7447	0.7447	8.7
0.7441	0.7441	8.8
0.7434	0.7434	8.9
0.7428	0.7428	9
0.7421	0.7421	9.1
0.7415	0.7415	9.2
0.7409	0.7409	9.3
0.7403	0.7403	9.4
0.7397	0.7397	9.5
0.7391	0.7391	9.6
0.7385	0.7385	9.7
0.7379	0.7379	9.8
0.7373	0.7373	9.9
0.7367	0.7367	10
0.7312	0.7312	11
0.7261	0.7261	12
0.7213	0.7213	13
0.7169	0.7169	14
0.7127	0.7127	15
0.7087	0.7087	16
0.7050	0.7050	17
0.7015	0.7015	18
0.6981	0.6981	19
0.6949	0.6949	20
0.6918	0.6918	21
0.6889	0.6889	22
0.6861	0.6861	23
0.6834	0.6834	24
0.6807	0.6807	25
0.6782	0.6782	26
0.6758	0.6758	27
0.6734	0.6734	28
0.6712	0.6712	29
0.6690	0.6690	30
0.6668	0.6668	31
0.6648	0.6648	32
0.6627	0.6627	33
0.6608	0.6608	34
0.6589	0.6589	35
0.6570	0.6570	36
0.6552	0.6552	37
0.6534	0.6534	38
0.6517	0.6517	39
0.6500	0.6500	40
0.6484	0.6484	41
0.6468	0.6468	42
0.6452	0.6452	43

0.6437	0.6437	44
0.6422	0.6422	45
0.6407	0.6407	46
0.6393	0.6393	47
0.6379	0.6379	48
0.6365	0.6365	49
0.6351	0.6351	50
0.6338	0.6338	51
0.6325	0.6325	52
0.6312	0.6312	53
0.6299	0.6299	54
0.6287	0.6287	55
0.6275	0.6275	56
0.6263	0.6263	57
0.6251	0.6251	58
0.6240	0.6240	59
0.6228	0.6228	60
0.6217	0.6217	61
0.6206	0.6206	62
0.6195	0.6195	63
0.6184	0.6184	64
0.6174	0.6174	65
0.6164	0.6164	66
0.6153	0.6153	67
0.6143	0.6143	68
0.6133	0.6133	69
0.6124	0.6124	70
0.6114	0.6114	71
0.6104	0.6104	72
0.6095	0.6095	73
0.6086	0.6086	74
0.6077	0.6077	75
0.6068	0.6068	76
0.6059	0.6059	77
0.6050	0.6050	78
0.6041	0.6041	79
0.6033	0.6033	80
0.6024	0.6024	81
0.6016	0.6016	82
0.6008	0.6008	83
0.6000	0.6000	84
0.5991	0.5991	85
0.5984	0.5984	86
0.5976	0.5976	87
0.5968	0.5968	88
0.5960	0.5960	89
0.5953	0.5953	90
0.5945	0.5945	91
0.5938	0.5938	92
0.5930	0.5930	93
0.5923	0.5923	94
0.5916	0.5916	95
0.5909	0.5909	96
0.5902	0.5902	97
0.5895	0.5895	98
0.5888	0.5888	99
0.5881	0.5881	100
0.5816	0.5816	110
0.5757	0.5757	120
0.5703	0.5703	130

0.5653	0.5653	140
0.5607	0.5607	150
0.5563	0.5563	160
0.5523	0.5523	170
0.5485	0.5485	180
0.5449	0.5449	190
0.5416	0.5416	200
0.5384	0.5384	210
0.5354	0.5354	220
0.5325	0.5325	230
0.5297	0.5297	240
0.5271	0.5271	250
0.5246	0.5246	260
0.5222	0.5222	270
0.5199	0.5199	280
0.5177	0.5177	290
0.5156	0.5156	300
0.5136	0.5136	310
0.5116	0.5116	320
0.5098	0.5098	330
0.5079	0.5079	340
0.5062	0.5062	350
0.5045	0.5045	360
0.5028	0.5028	370
0.5012	0.5012	380
0.4997	0.4997	390
0.4982	0.4982	400
0.4967	0.4967	410
0.4953	0.4953	420
0.4940	0.4940	430
0.4926	0.4926	440
0.4914	0.4914	450
0.4901	0.4901	460
0.4889	0.4889	470
0.4877	0.4877	480
0.4865	0.4865	490
0.4854	0.4854	500
0.4755	0.4755	600
0.4675	0.4675	700
0.4609	0.4609	800
0.4553	0.4553	900
0.4506	0.4506	1000

Appendix B. Matlab program: Creep strain

```
%%%%%%%%%%%%%%%%%%%%%%%%%%%%%%%%%%%%%%%%%%%%%%%%%%%%%%%%%%%%%%%%%%%%%%%%%%%%%%%
%%                                                                             %%
%%  MATLAB PROGRAM TO CALCULATE CREEP STRAIN WITH SUPERPOSITION                %%
%%  METHOD ACCORDING TO Cederwall, K. (2000) AND                               %%
%%  Comité Euro-International du Beton (1991)                                  %%
%%                                                                             %%
%%  PROGRAMMED BY:                                                             %%
%%                 CANOVIC SENAD                                               %%
%%                 GONCALVES JOAKIM                                            %%
%%                                      GOTHENBURG,SWEDEN 2004 ©               %%
%%                                                                             %%
%%%%%%%%%%%%%%%%%%%%%%%%%%%%%%%%%%%%%%%%%%%%%%%%%%%%%%%%%%%%%%%%%%%%%%%%%%%%%%%
clear all
clc

%% Input for creep coefficient calculations:

%% Age of concrete when loaded. [Days]
t0=1;
%% Age of concrete when analysis ends. [Days]
t=22;
%% Time between calculations. [Days]
deltat=0.1;
%% Relative humidity in surroundings. [%]
RH=75;
% h=2*Ac/u; (Mean value for all segments taken from Excel.)
h=0.704;
% Compressive strength of concrete according to tests for K70. [MPa]
fc=[96.6, 91.0, 83.4, 80.1, 97.1, 90.5, 93.4, 97.1]; %


%% Input for further creep and strain calculations:

%% Stress [Pa]
sigma=1E6;
%% Stress further applied [Pa]
deltasigma1=1e6;
%% Time when stress is changed [Days]
t1=8;
%% Stress further applied [Pa]
deltasigma2=-2e6;
%% Time when stress is changed [Days]
t2=15;
%% Young's modulus. [Pa]
Ec=2.2326E10;


%% Calculation of creep coefficient:

T=(t0:deltat:t)';
T0=1*(ones(size(t)));
fcm=mean(fc);
Bt0=1/(0.1+t0^0.2);
Bfcm=5.3/(fcm/10)^0.5;
FiRH=1+(1-(RH/100))/(0.46*(h/0.1)^3);
Fi0=FiRH*Bfcm*Bt0;
```

```
bh=150*(1+(1.2*RH/100)^18)*h/0.1+250;
if bh>1500
    bh=1500;
end
BH=bh*(ones(size(T)));
Bc=((T-T0)./(BH+(T-T0))).^0.3;
Fi=Fi0*Bc;




%% Calculation of creep strain

%% Time from beginning to end.
T1=(t0:deltat:t);
%% Time from first change of stress to end.
T2=(t1:deltat:t);
%% Time from beginning to first change of stress.
T3=(t0:deltat:t1-deltat);
%% Time from beginning to second change of stress.
T4=(t0:deltat:t2-deltat);
%% Time from second change of stress to end.
T5=(t2:deltat:t);

SIGMA1=sigma*(ones(size(T1)))';
SIGMA2=[zeros(size(T3)) deltasigma1*(ones(size(T2)))]';
SIGMA3=[zeros(size(T4)) deltasigma2*(ones(size(T5)))]';

epscc1=SIGMA1.*Fi/Ec;
Fi2=[zeros(size(T3)) Fi(1:size(T2,2))']';
epscc2=SIGMA2.*Fi2/Ec;
Fi3=[zeros(size(T4)) Fi(1:size(T5,2))']';
epscc3=SIGMA3.*Fi3/Ec;
epscctot=epscc1+epscc2+epscc3
tplot=(0:deltat:t-1)';
plot(tplot,epscctot),hold on
```

Appendix C. Matlab program: Young's Modulus

```
%%%%%%%%%%%%%%%%%%%%%%%%%%%%%%%%%%%%%%%%%%%%%%%%%%%%%%%%%%%%%%%%%%%%%%%%%%%%%%%
%%                                                                             %%
%%  MATLAB PROGRAM TO CALCULATE THE DEVELOPMENT OF YOUNG'S MODULUS             %%
%%  ACCORDING TO Comité Euro-International du Beton (1991).                    %%
%%                                                                             %%
%%  PROGRAMMED BY:                                                             %%
%%                 CANOVIC SENAD                                               %%
%%                 GONCALVES JOAKIM                                            %%
%%                                      GOTHENBURG,SWEDEN 2004 ©               %%
%%                                                                             %%
%%%%%%%%%%%%%%%%%%%%%%%%%%%%%%%%%%%%%%%%%%%%%%%%%%%%%%%%%%%%%%%%%%%%%%%%%%%%%%%
clear all
clc

%% INPUT DATA:

t=1:500;
s=0.25;

%% COMPRESSIVE STRENGTH OF CONCRETE, K70
%% ACCORDING TO MEASUREMENTS
x=[96.6, 91.0, 83.4, 80.1, 97.1, 90.5, 93.4, 97.1];

%% COMPRESSIVE STRENGTH OF CONCRETE, K45
%% ACCORDING TO MEASUREMENTS
%%x=[73.5, 75.4, 69.8];

%% CONSTANTS:
alfae=2.15*10^10;
fcm0=10*10^6;

%% ANALYSIS:

fcm=mean(x)*10^6;
ec=alfae*(fcm/fcm0)^(1/3);
ecs=0.85*ec;
t1=ones(size(t));
s1=s*t1;
betacct=exp(s1.*(1-sqrt(28./(t./t1))));
betaet=sqrt(betacct);
ect=betaet*ecs
plot(t, ect);,hold on
```

Appendix D. Material properties

The following material properties are taken from Boverket (1994) and they are given with characteristic values. These characteristic values can be used in design but were not used in the FE model. These values are presented here in order to get an overview of the material properties for the different strength classes used in the bridge.

Concrete Strength class values

The characteristic value for compressive strength in concrete denotes 85 % of the lower 5-percentile for compressive strength tests. The value for characteristic tensile strength can be chosen if compressive strength tests have been performed. The characteristic value for Young's modulus corresponds to the lower 30-percentile. The thermal expansion coefficient can be assumed to be $1,0*10^{-5}$ per °C for concrete.

K70:

Compressive strength,	$f_{cck} = 49,5$ Mpa
Tensile strength,	$f_{ctk} = 2,60$ MPa
Young's modulus,	$E_{ck} = 37,5$ MPa
Thermal expansion coefficient,	$\alpha_c = 1,0*10^{-5}$ per °C

K40:

Compressive strength,	$f_{cck} = 28,5$ MPa
Tensile strength,	$f_{ctk} = 1,95$ MPa
Young's modulus,	$E_{ck} = 32,0$ MPa
Thermal expansion coefficient,	$\alpha_c = 1,0*10^{-5}$ per °C

K45:

Compressive strength,	$f_{cck} = 32,0$ MPa
Tensile strength,	$f_{ctk} = 2,10$ MPa
Young's modulus,	$E_{ck} = 33,0$ MPa
Thermal expansion coefficient,	$\alpha_c = 1,0*10^{-5}$ per °C

Reinforcement Strength class values

The characteristic value for yield strength in reinforcement corresponds to the lower 5-percentile for strength tests performed. Young's modulus for reinforcement that is not prestressed can be assumed to be 200 GPa if nothing else can be shown. The thermal expansion coefficient can be assumed to be $1,0*10^{-5}$ per °C.

K 500:

Yield strength,	$f_{yk} = 500$ MPa
Young's modulus,	$E_{sk} = 200$ GPa
Thermal expansion coefficient,	$\alpha_s = 1,0*10^{-5}$ per °C

Ks 60 S:

Yield strength,	f_{yk} = 590 - 620 MPa
Young's modulus,	E_{sk} = 200 GPa
Thermal expansion coefficient,	$\alpha_s = 1{,}0*10^{-5}$ per °C

Appendix E. Construction schedule.

In following pages a schedule for the construction events of the arch is shown. The abbreviations in the schedule are explained below.

Arch segments:

Sxx = Swedish arch segment xx.
Nxx = Norwegian arch segment xx.

Supporting pylon parts:

S = Swedish side.
N = Norwegian side.
LOW = Lower part.
MID = Middle part.
UP = Upper part.

Supporting tendons:

SW = Swedish side.
NW = Norwegian side.
TP = Tendon between rock and temporary supporting pylon.
AR = Tendon between arch and temporary supporting pylon.
TST = Transverse tendon between rock and arch.
R = Right side of the arch.
L = Left side of the arch.

Lnn, nn = Number of strands in tendon.

IN xx = Introducing a new tendon, with the initial force xx bar.
IF xx = Increase of force to xx bar.
DE xx = Decrease of force to xx bar.
nn—mm = Removal of mm strands from the total amount of nn strands in a tendon.
RT= Total removal of tendon

CONSTRUCTION DATE		2003-05-15	2003-06-09	2003-06-18	2003-06-19	2003-07-02	2003-07-14	2003-07-23	2003-07-24	2003-07-26	2003-08-04	2003-08-11	2003-08-13	2003-08-17	2003-08-21	2003-08-23	2003-08-27	2003-09-01	2003-09-09	2003-09-10	2003-09-11	2003-09-13	2003-09-18	2003-09-19	2003-09-25	2003-09-27	2003-10-06	2003-10-15	2003-10-16	2003-10-21	2003-10-27	2003-11-03	2003-11-05	2003-11-10	2003-11-12	2003-11-13	2003-11-15	2003-11-17	2003-11-18	2003-11-20	2003-11-21	2003-11-24	2003-11-27	2003-11-28	2003-12-01	2003-12-03	2003-12-04	2003-12-05	2003-12-06
ARCH-SEGMENTS		S-ABUT	S1.1	N-ABUT	S1.2	S2	S3	N1.1		S4	N1.2	S5	N2			N3		N4	N5			S6		N6	S7		N7		S8	N8	S9	N9	S10	N10	S11		N11		S12		N12	S13		N13	S14	N14			S15
PYLON PARTS								S.LOW						N.LOW																S.MID		N.MID																
LOWER PYLON CABLES																																																
	SW-TP-01R	L22								IN 100				IF 130											IF 240																							22--5	
	SW-TP-01L	L22								IN 100				IF 205							DE 195				IF 210																							22--5	
	SW-TP-02R	L19								IN 105													IF 120				IF 270						19--8														RT	
	SW-TP-02L	L19								IN 105										IF 150							IF 270						19--8														RT	
	SW-AR-01R	L19								IN 260																							19--9														RT	
	SW-AR-01L	L19								IN 260																							19--9														RT	
	SW-AR-02R	L12												IN 87											IF 340																								
	SW-AR-02L	L12												IN 233							IF 291				IF 340																								
	SW-AR-03R	L15																									IN 200																							
	SW-AR-03L	L15																									IN 200																							
MIDDLE PYLON CABLES																																																	
	SW-TP-03R	L22																													IN 70		IF 115							IF 217		IF 312						
	SW-TP-03L	L22																													IN 70		IF 115							IF 217		IF 312						
	SW-TP-04R	L22																													IN 68						IF 247										IF 346	
	SW-TP-04L	L22																													IN 68						IF 247										IF 346	
	SW-AR-04R	L12																													IN 190																	
	SW-AR-04L	L12																													IN 190																	
	SW-AR-05R	L12																																			IN 197											
	SW-AR-05L	L12																																			IN 197											
	SW-AR-06R	L12																																									IN 180					
	SW-AR-06L	L12																																									IN 180					
	SW-AR-07R	L9																																														IN 178	
	SW-AR-07L	L9																																														IN 178	
	SW-TP-05R	L15																																														IN 50	
	SW-TP-05L	L15																																														IN 50	
	SW-AR-08R	L9																																															
	SW-AR-08L	L9																																															
UPPER PYLON CABLES																																																	
	SW-TP-06R	L22																																															
	SW-TP-06L	L22																																															
	SW-TP-07R	L22																																															
	SW-TP-07L	L22																																															
	SW-AR-09R	L9																																															
	SW-AR-09L	L9																																															
	SW-AR-10R	L9																																															
	SW-AR-10L	L9																																															
	SW-AR-11R	L9																																															
	SW-AR-11L	L9																																															
	SW-TP-08R	L22																																															
	SW-TP-08L	L22																																															
	SW-AR-12R	L12																																															
	SW-AR-12L	L12																																															
	SW-AR-13R	L12																																															
	SW-AR-13L	L12																																															
	SW-TP-09R	L22																																															
	SW-TP-09L	L22																																															
	SW-AR-14R	L12																																															
	SW-AR-14L	L12																																															
	SW-TP-10R	L22																																															
	SW-TP-10L	L22																																															
	SW-AR-15R	L12																																															
	SW-AR-15L	L12																																															
	SW-AR-16R	L15																																															
	SW-AR-16L	L15																																															
	SW-TP-11R	L22																																															
	SW-TP-11L	L21																																															
	SW-AR-17R	L15																																															
	SW-AR-17L	L15																																															
TRANSVERSE CABLES																																																
	SW-TST-01L	L22																																															
	SW-TST-01R	L22																																															
LOWER PYLON CABLES																																																
	NW-TP-01R	L22													IN 24		IF 90						IF 240																									22--5	
	NW-TP-01L	L22													IN 24		IF 90						IF 240																									22--5	
	NW-TP-02R	L19															IN 100									IF 230		IF 275						19--8														RT	
	NW-TP-02L	L19															IN 100									IF 230		IF 275						19--8														RT	
	NW-AR-01R	L19															IN 250																	19--9														RT	
	NW-AR-01L	L19															IN 250																	19--9														RT	
	NW-AR-02R	L12																					IN 290																										
	NW-AR-02L	L12																					IN 290																										
	NW-AR-03R	L15																									IN 200																							15--7	
	NW-AR-03L	L15																									IN 200																							15--7	
MIDDLE PYLON CABLES																																																	
	NW-TP-03R	L22																															IN 70	IF 105	IF 135							IF 295						
	NW-TP-03L	L22																															IN 70	IF 108	IF 135							IF 295						
	NW-TP-04R	L22																															IN 60		IF 80						IF 180								
	NW-TP-04L	L22																															IN 60		IF 80						IF 180								
	NW-AR-04R	L12																															IN 195		IF 305														
	NW-AR-04L	L12																															IN 195		IF 305														
	NW-AR-05R	L12																																							IN 192								
	NW-AR-05L	L12																																							IN 192								
	NW-AR-06R	L12																																													IN 182		
	NW-AR-06L	L12																																													IN 182		
	NW-AR-07R	L9																																														IN 183	
	NW-AR-07L	L9																																														IN 183	
	NW-TP-05R	L15																																														IN 50	
	NW-TP-05L	L15																																														IN 50	
	NW-AR-08R	L9																																															
	NW-AR-08L	L9																																															
UPPER PYLON CABLES																																																
	NW-TP-06R	L19																																															
	NW-TP-06L	L19																																															
	NW-TP-07R	L19																																															
	NW-TP-07L	L19																																															
	NW-TP-08R	L19																																															
	NW-TP-08L	L19																																															
	NW-TP-09R	L19																																															
	NW-TP-09L	L19																																															
	NW-TP-10R	L19																																															
	NW-TP-10L	L19																																															
	NW-TP-11R	L19																																															
	NW-TP-11L	L19																																															
	NW-AR-09R	L9																																															
	NW-AR-09L	L9																																															
	NW-AR-10R	L9																																															
	NW-AR-10L	L9																																															
	NW-AR-11R	L9																																															
	NW-AR-11L	L9																																															
	NW-AR-12R	L12																																															
	NW-AR-12L	L12																																															
	NW-AR-13R	L12																																															
	NW-AR-13L	L12																																															
	NW-AR-14R	L12																																															
	NW-AR-14L	L12																																															
	NW-AR-15R	L12																																															
	NW-AR-15L	L12																																															
	NW-AR-16R	L15																																															
	NW-AR-16L	L15																																															
	NW-AR-17R	L15																																															
	NW-AR-17L	L15																																															
TRANSVERSE CABLES																																																
	NW-TST-01R	L22																																															
	NW-TST-01L	L22																																															

2003-12-09	2003-12-10	2003-12-11	2003-12-13	2003-12-14	2003-12-15	2003-12-16	2003-12-17	2003-12-18	2003-12-19	2003-12-20	2004-01-06	2004-01-08	2004-01-09	2004-01-10	2004-01-13	2004-01-14	2004-01-15	2004-01-16	2004-01-17	2004-01-19	2004-01-20	2004-01-22	2004-01-23	2004-01-24	2004-01-26	2004-01-29	2004-01-31	2004-02-01	2004-02-02	2004-02-04	2004-02-05	2004-02-07	2004-02-09	2004-02-10	2004-02-11	2004-02-12	2004-02-15	2004-02-16	2004-02-17	2004-02-18	2004-02-19	2004-02-22	2004-02-23	2004-03-07	2004-03-15	2004-09-01		CABLES & SEGMENTS	
	S16 N15		N16		S17				N17	S18			N18	S19		S20	N19			S21	N20			S22	N21	S23	N22				S24	N23		S25		N24			N25			N26					ARCH-SEGMENT	
		S.UP			N.UP																																													
																																																LOWER PYLON CABLES	
				17--5																																									RT		LOWER PYLON CABLES	SW-TP-01R	L22
				17--5																																									RT			SW-TP-01L	L22
																																																SW-TP-02R	L19
																																																SW-TP-02L	L19
																																																SW-AR-01R	L19
																																																SW-AR-01L	L19
																																													RT			SW-AR-02R	L12
																																													RT			SW-AR-02L	L12
				RT																																											SW-AR-03R	L15
				RT																																											SW-AR-03L	L15
																																																MIDDLE PYLON CABLES	
																			22--16																								RT				SW-TP-03R	L22
																			22--16																								RT				SW-TP-03L	L22
																						22--6											16--10									RT				SW-TP-04R	L22
																						22--6											16--10									RT				SW-TP-04L	L22
																													12--6					RT													SW-AR-04R	L12
																													12--6					RT													SW-AR-04L	L12
																			12--9																								RT				SW-AR-05R	L12
																			12--9																								RT				SW-AR-05L	L12
																																												RT				SW-AR-06R	L12
																																												RT				SW-AR-06L	L12
																																												RT				SW-AR-07R	L9
																																												RT				SW-AR-07L	L9
IF 253																													15--8					RT													SW-TP-05R	L15
IF 253																													15--8					RT													SW-TP-05L	L15
IN 307																																		RT													SW-AR-08R	L9
IN 307																																		RT													SW-AR-08L	L9
																																																UPPER PYLON CABLES	
			IN 107						IF 240									IF 300																									RT					UPPER PYLON CABLES	SW-TP-06R	L22
			IN 107						IF 240									IF 300																									RT					SW-TP-06L	L22
									IN 70			IF 245																															RT					SW-TP-07R	L22
									IN 70			IF 245																															RT					SW-TP-07L	L22
			IN 161																																								RT					SW-AR-09R	L9
			IN 161																																								RT					SW-AR-09L	L9
									IN 249																															9--6			RT					SW-AR-10R	L9
									IN 249																															9--6			RT					SW-AR-10L	L9
												IN 195																												RT							SW-AR-11R	L9
												IN 195																												RT							SW-AR-11L	L9
															IN 226			IF 310																									RT					SW-TP-08R	L22
															IN 226			IF 310																									RT					SW-TP-08L	L22
															IN 213																									RT							SW-AR-12R	L12
															IN 213																									RT							SW-AR-12L	L12
																		IN 193																						12--10			RT					SW-AR-13R	L12
																		IN 193																						12--10			RT					SW-AR-13L	L12
																						IN 158						IF 269															RT					SW-TP-09R	L22
																						IN 158						IF 269															RT					SW-TP-09L	L22
																						IN 216																					RT					SW-AR-14R	L12
																						IN 216																					RT					SW-AR-14L	L12
																									IN 246	IF 270																	RT					SW-TP-10R	L22
																									IN 246	IF 270																	RT					SW-TP-10L	L22
																									IN 252	IF 275																	RT					SW-AR-15R	L12
																									IN 252	IF 275																	RT					SW-AR-15L	L12
																												IN 140															RT					SW-AR-16R	L15
																												IN 140															RT					SW-AR-16L	L15
																																	IN 202										RT					SW-TP-11R	L22
																																	IN 212										RT					SW-TP-11L	L21
																																	IN 263							DE 220	IF 240 15--3		RT					SW-AR-17R	L15
																																	IN 263							DE 220	IF 240 15--3		RT					SW-AR-17L	L15
																																																TRANSVERSE CABLES	
						IN 80 13L					IF 80 22L												IF 180																							RT		SW-TST-01L	L22
						IN 80 13L					IF 80 22L												IF 180																							RT		SW-TST-01R	L22
																																																LOWER PYLON CABLES	
							17--10																																						RT		LOWER PYLON CABLES	NW-TP-01R	L22
							17--10																																						RT			NW-TP-01L	L22
																																																NW-TP-02R	L19
																																																NW-TP-02L	L19
																																																NW-AR-01R	L19
																																																NW-AR-01L	L19
																																													RT			NW-AR-02R	L12
																																													RT			NW-AR-02L	L12
							RT																																								NW-AR-03R	L15
							RT																																								NW-AR-03L	L15
																																																MIDDLE PYLON CABLES	
																										RT																11L IN 80		RT			MIDDLE PYLON CABLES	NW-TP-03R	L22
																										RT																11L IN 80		RT				NW-TP-03L	L22
																														22--10												6L DF 80		RT				NW-TP-04R	L22
																														22--10												6L DF 80		RT				NW-TP-04L	L22
																								12--6																				RT				NW-AR-04R	L12
																								12--6																				RT				NW-AR-04L	L12
																										RT																					NW-AR-05R	L12
																										RT																					NW-AR-05L	L12
																																												RT				NW-AR-06R	L12
																																												RT				NW-AR-06L	L12
																																												RT				NW-AR-07R	L9
																																												RT				NW-AR-07L	L9
		IF 197																						15--8																				RT				NW-TP-05R	L15
		IF 197																						15--8																				RT				NW-TP-05L	L15
		IN 294																												RT																	NW-AR-08R	L9
		IN 294																												RT																	NW-AR-08L	L9
																																																UPPER PYLON CABLES	
						IN 107					IF 206												IF 250																				RT				UPPER PYLON CABLES	NW-TP-06R	L19
						IN 107					IF 206												IF 250																				RT					NW-TP-06L	L19
											IN 50					IF 214																											RT					NW-TP-07R	L19
											IN 50					IF 214																											RT					NW-TP-07L	L19
																				IN 178			IF 245																				RT					NW-TP-08R	L19
																				IN 178			IF 245																				RT					NW-TP-08L	L19
																										IN 158																	RT					NW-TP-09R	L19
																										IN 158																	RT					NW-TP-09L	L19
																														IN 228													RT					NW-TP-10R	L19
																														IN 228													RT					NW-TP-10L	L19
																																						IN 227					RT					NW-TP-11R	L19
																																						IN 227					RT					NW-TP-11L	L19
						IN 196																																					RT					NW-AR-09R	L9
						IN 196																																					RT					NW-AR-09L	L9
											IN 217																											9--6					RT					NW-AR-10R	L9
											IN 217																											9--6					RT					NW-AR-10L	L9
																IN 218																			RT													NW-AR-11R	L9
																IN 218																			RT													NW-AR-11L	L9
																				IN 206															RT													NW-AR-12R	L12
																				IN 206															RT													NW-AR-12L	L12
																							IN 245															12--10					RT					NW-AR-13R	L12
																							IN 245															12--10					RT					NW-AR-13L	L12
																										IN 221																	RT					NW-AR-14R	L12
																										IN 221																	RT					NW-AR-14L	L12
																														IN 258													RT					NW-AR-15R	L12
																														IN 258													RT					NW-AR-15L	L12
																																			IN 130								RT					NW-AR-16R	L15
																																			IN 130								RT					NW-AR-16L	L15
																																					IN 262			IF 330			RT					NW-AR-17R	L15
																																					IN 262			IF 330			RT					NW-AR-17L	L15
																																																TRANSVERSE CABLES	
								18L IN 80																																						RT		NW-TST-01R	L22
								18L IN 80																																12L IF 180						RT		NW-TST-01L	L22

Appendix F. ABAQUS input files for analysis steps.

In the following pages three randomly chosen events show how the three different categorys of construction events were programmed in the input file for abaqus.

Category 1: New segment

```
**************************ACTIVATING OF ELEMENTS IN 150503**************
*STEP
      ACTIVATING OF ELEMENTS: CONSTRUCTION 150503
*STATIC
      0, 1
*FIELD, VARIABLE=1
NALL, 1.
*MODEL CHANGE, ADD, TYPE=ELEMENT
SWEABUT
*TEMPERATURE, AMPLITUDE=TEMP
NALL, 1
*END STEP
************************LOADING WITH SELF WEIGHT, 160503***************
*STEP
      SELF WEIGHT: 160503
*STATIC
      0, 10E-20
*DLOAD
      CON_150503, GRAV, 10, 0, 0, 1
*TEMPERATURE, AMPLITUDE=TEMP
NALL, 1
*OUTPUT, FIELD
*NODE OUTPUT
      U,RF
*ELEMENT OUTPUT, POSITION=CENTROIDAL, ELSET=CON_150503
      SF
*ELEMENT OUTPUT, POSITION=INTEGRATION POINTS, ELSET=CON_150503
      S, CE
*END STEP
****************************CREEPING FROM 160503************************
*STEP
      CREEPING FROM 160503
*VISCO , CETOL=1E-5
1E-5, 24 , 1E-20, 1
*FIELD, VARIABLE=1
NALL, 2.
*TEMPERATURE, AMPLITUDE=TEMP
NALL, 1
*OUTPUT, FIELD
*NODE OUTPUT
      U,RF
*ELEMENT OUTPUT, POSITION=CENTROIDAL, ELSET=CON_150503
      SF
*ELEMENT OUTPUT, POSITION=INTEGRATION POINTS, ELSET=CON_150503
      S, CE
*END STEP
```

Category 2: Tendon modification

```
************************ACTIVATING OF ELEMENTS IN 040204**********************
*STEP
   ACTIVATING OF ELEMENTS: CONSTRUCTION 040204
*STATIC
      0, 10E-20
*MODEL CHANGE, ADD, TYPE=ELEMENT
      NWTP10R, NWTP10L, NWAR15R, NWAR15L
*MODEL CHANGE, REMOVE, TYPE=ELEMENT
      NWTP04R3, NWTP04L3, NWAR08R1, NWAR08L1
*TEMPERATURE, AMPLITUDE=TEMP
NALL, 1
*OUTPUT, FIELD
*NODE OUTPUT
      U,RF
*ELEMENT OUTPUT, POSITION=CENTROIDAL, ELSET=CON_040204
      SF
*ELEMENT OUTPUT, POSITION=INTEGRATION POINTS, ELSET=CON_040204
      S, CE
*END STEP
***********************LOADING WITH SELF WEIGHT, 040204************************
*STEP
      SELF WEIGHT: 040204
*STATIC
      0, 10E-20
*DLOAD
      NWTP10R, GRAV, 10, 0, 0, 1
      NWTP10L, GRAV, 10, 0, 0, 1
      NWAR15R, GRAV, 10, 0, 0, 1
      NWAR15L, GRAV, 10, 0, 0, 1
*TEMPERATURE, AMPLITUDE=TEMP
NALL, 1
*OUTPUT, FIELD
*NODE OUTPUT
      U,RF
*ELEMENT OUTPUT, POSITION=CENTROIDAL, ELSET=CON_040204
      SF
*ELEMENT OUTPUT, POSITION=INTEGRATION POINTS, ELSET=CON_040204
      S, CE
*END STEP
*****************************CREEPING FROM 040204***************************
*STEP
      CREEPING FROM 040204
*VISCO , CETOL=1E-5
1E-5, 1 , 1E-20, 1
*FIELD, VARIABLE=1
NALL, 113.
*TEMPERATURE, AMPLITUDE=TEMP
NALL, 1
*OUTPUT, FIELD
*NODE OUTPUT
      U,RF
*ELEMENT OUTPUT, POSITION=CENTROIDAL, ELSET=CON_040204
      SF
*ELEMENT OUTPUT, POSITION=INTEGRATION POINTS, ELSET=CON_040204
      S, CE
*END STEP
```

Category 3: New segment and tendon modification

```
************************ACTIVATING OF ELEMENTS IN 290104***************
*STEP
   ACTIVATING OF ELEMENTS: CONSTRUCTION 290104_1
*STATIC
      0, 10E-20
*MODEL CHANGE, ADD, TYPE=ELEMENT
      SWTP10R1, SWTP10L1, SWAR15R1, SWAR15L1, NWTP09R, NWTP09L, NWAR14R,
NWAR14L
*MODEL CHANGE, REMOVE, TYPE=ELEMENT
      SWTP10R, SWTP10L, SWAR15R, SWAR15L, NWTP03R5, NWTP03L5, NWAR05R1,
NWAR05L1
*TEMPERATURE, AMPLITUDE=TEMP
NALL, 1
*OUTPUT, FIELD
*NODE OUTPUT
      U,RF
*ELEMENT OUTPUT, POSITION=CENTROIDAL, ELSET=CON_290104_1
      SF
*ELEMENT OUTPUT, POSITION=INTEGRATION POINTS, ELSET=CON_290104_1
      S, CE
*END STEP
*********************LOADING WITH SELF WEIGHT, 290104**********************
*STEP
      SELF WEIGHT: 290104_1
*STATIC
      0, 10E-20
*DLOAD
      SWTP10R1,  GRAV, 10, 0, 0, 1
      SWTP10L1,  GRAV, 10, 0, 0, 1
      SWAR15R1,  GRAV, 10, 0, 0, 1
      SWAR15L1,  GRAV, 10, 0, 0, 1
      NWTP09R,   GRAV, 10, 0, 0, 1
      NWTP09L,   GRAV, 10, 0, 0, 1
      NWAR14R,   GRAV, 10, 0, 0, 1
      NWAR14L,   GRAV, 10, 0, 0, 1
*TEMPERATURE, AMPLITUDE=TEMP
NALL, 1
*OUTPUT, FIELD
*NODE OUTPUT
      U,RF
*ELEMENT OUTPUT, POSITION=CENTROIDAL, ELSET=CON_290104_1
      SF
*ELEMENT OUTPUT, POSITION=INTEGRATION POINTS, ELSET=CON_290104_1
      S, CE
*END STEP
*********************ACTIVATING OF ELEMENTS IN 290104************************
*STEP
   ACTIVATING OF ELEMENTS: CONSTRUCTION 290104_2
*VISCO , CETOL=1E-5
1E-5, 1 , 1E-20, 1
*FIELD, VARIABLE=1
NALL, 108.
*MODEL CHANGE, ADD, TYPE=ELEMENT
      SWESEG23
*TEMPERATURE, AMPLITUDE=TEMP
NALL, 1
```

```
*OUTPUT, FIELD
*NODE OUTPUT
      U,RF
*ELEMENT OUTPUT, POSITION=CENTROIDAL, ELSET=CON_290104_2
      SF
*ELEMENT OUTPUT, POSITION=INTEGRATION POINTS, ELSET=CON_290104_2
      S, CE
*END STEP
**********************LOADING WITH SELF WEIGHT, 300104**********************
*STEP
      SELF WEIGHT: 300104
*STATIC
      0, 10E-20
*DLOAD
      SWESEG23,  GRAV, 10, 0, 0, 1
*TEMPERATURE, AMPLITUDE=TEMP
NALL, 1
*OUTPUT, FIELD
*NODE OUTPUT
      U,RF
*ELEMENT OUTPUT, POSITION=CENTROIDAL, ELSET=CON_290104_2
      SF
*ELEMENT OUTPUT, POSITION=INTEGRATION POINTS, ELSET=CON_290104_2
      S, CE
*END STEP
************************CREEPING FROM 300104*****************************
*STEP
      CREEPING FROM 300104
*VISCO , CETOL=1E-5
1E-5, 1 , 1E-20, 1
*FIELD, VARIABLE=1
NALL, 109.
*TEMPERATURE, AMPLITUDE=TEMP
NALL, 1
*OUTPUT, FIELD
*NODE OUTPUT
      U,RF
*ELEMENT OUTPUT, POSITION=CENTROIDAL, ELSET=CON_290104_2
      SF
*ELEMENT OUTPUT, POSITION=INTEGRATION POINTS, ELSET=CON_290104_2
      S, CE
*END STEP
```

Appendix G. ABAQUS input file for temperature effect.

```
*****************************TEMPERATURE************************************
**
**                 TIME = DAYS
**          TEMPERATURE = DEGREES OF CELSIUS
**
**
*INITIAL CONDITIONS, TYPE=TEMPERATURE
NALL, 7.874684444
**
**
*AMPLITUDE, NAME=TEMP, TIME=TOTAL TIME, DEFINITION=TABULAR
0   , 7.874684444 , 1   , 7.883919722 , 2   , 8.666080625 , 3   , 12.31819292
4   , 10.77513813 , 5   , 9.361523125 , 6   , 9.802428681 , 7   , 10.74423354
8   , 9.185870208 , 9   , 11.49138792 , 10  , 13.59840278 , 11  , 12.74277771
12  , 12.19104146 , 13  , 12.1173591  , 14  , 12.81534597 , 15  , 14.85791667
16  , 14.88972215 , 17  , 16.1575     , 18  , 17.31069444 , 19  , 18.04708333
20  , 17.969375   , 21  , 16.82979167 , 22  , 15.09729167 , 23  , 14.85958333
24  , 15.87784722 , 25  , 14.66402778 , 26  , 15.10645833 , 27  , 13.45673611
28  , 15.29375    , 29  , 15.18388889 , 30  , 15.51479167 , 31  , 13.56909708
32  , 13.67048472 , 33  , 15.69215278 , 34  , 16.39104167 , 35  , 15.58305556
36  , 15.92083333 , 37  , 14.87166667 , 38  , 15.565      , 39  , 12.54166667
40  , 13.54451389 , 41  , 17.56736111 , 42  , 19.54819444 , 43  , 19.91840278
44  , 18.2925     , 45  , 16.20840278 , 46  , 15.09854167 , 47  , 14.97763889
48  , 14.95076389 , 49  , 17.46138889 , 50  , 17.40631944 , 51  , 18.31083333
52  , 18.680625   , 53  , 16.41944444 , 54  , 16.83861111 , 55  , 17.10611111
56  , 17.75520833 , 57  , 15.47902778 , 58  , 16.92145833 , 59  , 18.90680556
60  , 20.90527778 , 61  , 23.99055556 , 62  , 25.08743056 , 63  , 23.23159722
64  , 20.46583333 , 65  , 18.41722222 , 66  , 19.81555556 , 67  , 20.41826389
68  , 18.3675     , 69  , 18.34486111 , 70  , 19.29895833 , 71  , 17.35548611
72  , 17.51048611 , 73  , 16.20458333 , 74  , 17.54375    , 75  , 17.78104167
76  , 17.76041667 , 77  , 19.53409722 , 78  , 20.07409722 , 79  , 18.55965278
80  , 18.28993056 , 81  , 18.86423611 , 82  , 18.81381944 , 83  , 18.48902778
84  , 19.97659722 , 85  , 21.20340278 , 86  , 20.45625    , 87  , 21.42826389
88  , 21.244375   , 89  , 21.25125    , 90  , 18.38881944 , 91  , 15.925
92  , 17.00854167 , 93  , 17.58590278 , 94  , 18.21493056 , 95  , 17.86145833
96  , 17.109375   , 97  , 17.89041667 , 98  , 16.033125   , 99  , 17.08333333
100 , 16.84423611 , 101 , 18.00708333 , 102 , 15.00736111 , 103 , 12.75666493
104 , 10.76999722 , 105 , 12.55451271 , 106 , 13.70229153 , 107 , 12.88242917
108 , 11.36409479 , 109 , 10.94142854 , 110 , 11.4685616  , 111 , 14.44173611
112 , 15.14409722 , 113 , 14.60444444 , 114 , 15.38458333 , 115 , 14.40979167
116 , 15.82097222 , 117 , 15.56763889 , 118 , 14.97618056 , 119 , 14.65159722
120 , 14.49694444 , 121 , 13.67986111 , 122 , 15.08375    , 123 , 16.36618056
124 , 15.09701389 , 125 , 12.37090139 , 126 , 16.14555556 , 127 , 13.34819444
128 , 9.429004653 , 129 , 14.08131944 , 130 , 15.77736111 , 131 , 11.33749819
132 , 9.518880139 , 133 , 14.02777778 , 134 , 13.03854167 , 135 , 8.802135972
136 , 6.159553264 , 137 , 7.747997986 , 138 , 9.156066458 , 139 , 12.15180556
140 , 9.928885417 , 141 , 10.91277674 , 142 , 9.415961944 , 143 , 6.628990139
144 , 7.130378611 , 145 , 7.229440903 , 146 , 6.262955625 , 147 , 7.104136181
148 , 10.72805354 , 149 , 9.0417675   , 150 , 7.86944875  , 151 , 4.898767986
152 , 4.107761676 , 153 , 4.397254403 , 154 , 3.657316242 , 155 , 3.789845708
156 , 2.059436897 , 157 , 1.232201204 , 158 , 0.125263889 , 159 , -0.066583292
```

160 , -1.698499819, 161 , -3.8393385 , 162 , 0.245375625 , 163 , 1.657110709
164 , -0.377368108, 165 , 6.345675457 , 166 , 10.12909333 , 167 , 5.73872625
168 , 2.976867639 , 169 , 3.062458125 , 170 , 5.041427778 , 171 , 6.153074236
172 , 8.091201597 , 173 , 5.867719444 , 174 , 8.329785417 , 175 , 7.531932014
176 , 5.969004236 , 177 , 2.544986111 , 178 , 2.329193958 , 179 , 4.239851528
180 , 2.886347222 , 181 , 1.620735694 , 182 , 0.914319535 , 183 , 4.72480375
184 , 3.511450556 , 185 , 4.302671458 , 186 , 1.107847194 , 187 , 1.959832439
188 , 7.101066319 , 189 , 5.052587639 , 190 , 2.506291667 , 191 , 1.250339944
192 , 0.002743128 , 193 , -1.200673501, 194 , -0.452652822, 195 , 2.377485583
196 , 4.548226319 , 197 , 4.041831111 , 198 , 4.330017083 , 199 , 4.5851225
200 , 5.756739792 , 201 , 5.1365875   , 202 , 4.609565694 , 203 , 6.232968681
204 , 5.448545903 , 205 , -0.108514055, 206 , 1.922735271 , 207 , 4.813088028
212 , 1.683624001 , 213 , 3.15482509 , 214 , 1.314673686 , 215 , -0.038909647
216 , 6.456205   , 217 , 7.176260139 , 218 , 6.588669931 , 219 , 1.361860142
220 , -1.774180256, 221 , -7.370571806, 222 , -8.48935875 , 223 , 5.271456181
236 , -2.687569444, 237 , -1.467402736, 238 , -1.083909625, 239 , 0.154763732
240 , -3.21299834 , 241 , 0.444888715 , 242 , 2.766041653 , 243 , 2.353611111
244 , 0.27589575 , 245 , -2.027680556, 246 , -3.641255556, 247 , -8.653257569
248 , -5.124610224, 249 , -3.467679479, 250 , -7.730341528, 251 , -11.70284576
252 , -9.290962847, 253 , -0.401951387, 254 , -0.015784965, 255 , -3.382236111
256 , -2.411444444, 257 , -2.959055556, 258 , -2.653090278, 259 , -1.748645833
260 , -2.647368056, 261 , -1.009847069, 262 , -3.773554278, 263 , 0.395117813
264 , 3.91997016 , 265 , 5.916594097 , 266 , 4.866400278 , 267 , 4.949580208
268 , 0.629867993 , 269 , -3.604048333, 270 , -4.268831514, 271 , -4.572711924
272 , -4.811060486, 273 , -0.822131451, 274 , -0.308930689, 275 , -0.295916588
276 , -0.858493076, 277 , -0.343597354, 278 , 1.810228406 , 279 , 0.483277067
280 , -1.63522779 , 281 , 1.380395715 , 282 , 1.636631992 , 283 , -0.947763622
284 , -1.604451278, 285 , 1.94812491 , 286 , 0.373395661 , 287 , -2.688623389
288 , -4.359345764, 289 , -3.180089722, 290 , -4.340247003, 291 , 1.164978085
292 , 1.69065875 , 293 , -2.63166566 , 294 , -5.542684653, 295 , -3.53020625
296 , -0.208020806, 297 , 0.765624375 , 298 , 1.07916628 , 299 , -0.258020077
300 , 0.293145366 , 301 , -0.850187583, 302 , -0.46169426 , 303 , -0.201798478
304 , 3.539242083 , 305 , 5.476740139 , 306 , 5.831294375 , 307 , 6.025356319
308 , 5.255087361 , 309 , 4.988399444 , 310 , 3.288408938 , 311 , 1.957061276
312 , 2.207416347 , 313 , 1.502812181 , 314 , 0.699215539 , 315 , 0.003486182
316 , -0.140743111, 321 , 6.577978319 , 322 , 5.264088542 , 323 , 2.96087364
324 , 3.212394124 , 325 , 5.477997246 , 326 , 5.911170069 , 327 , 4.525878889
328 , 4.259755208 , 329 , 6.299206111 , 330 , 5.391260146 , 331 , 5.391260146
332 , 4.737892194 , 333 , 4.987024694 , 334 , 3.389394215 , 335 , 5.692545486
336 , 5.666086042 , 337 , 7.609206389 , 338 , 9.8771525   , 339 , 11.99048472
340 , 12.0943725 , 341 , 8.932912639 , 342 , 7.679220347 , 343 , 7.3518445
344 , 8.52947375 , 345 , 9.109650347 , 346 , 8.600440486 , 347 , 7.835140278
348 , 8.928953056 , 349 , 9.624358472 , 350 , 9.268344653 , 351 , 10.30440701
352 , 11.96541389 , 353 , 10.89012944 , 354 , 10.84596771 , 355 , 10.83624708
356 , 14.23361111 , 357 , 16.14645833 , 358 , 18.72840278 , 359 , 18.04215278
360 , 18.13048611 , 361 , 15.99159722 , 362 , 10.00763458 , 363 , 8.852153958
364 , 8.886235208 , 365 , 11.42374757 , 366 , 10.84067806 , 367 , 11.61569986
368 , 13.06999785 , 369 , 12.98472222 , 370 , 12.8392359 , 371 , 9.892323403
372 , 8.466344792 , 373 , 7.703266944 , 374 , 9.276435208 , 375 , 10.74976951
376 , 9.795550764 , 377 , 9.795550764 , 378 , 11.66653236 , 379 , 10.85388431
380 , 10.50494215 , 381 , 13.50395611 , 382 , 14.27760292 , 383 , 14.18749785
384 , 15.99062319 , 385 , 15.56548479 , 386 , 12.58513882 , 387 , 13.5270809
388 , 15.08527778 , 389 , 14.62909722 , 390 , 12.34846986 , 391 , 13.38124826
392 , 15.42305486 , 393 , 15.203125   , 394 , 15.79673611 , 395 , 15.883125
396 , 16.739375   , 397 , 15.3684716 , 398 , 13.51055326 , 399 , 13.76416569
400 , 12.12826243 , 401 , 9.331760139 , 402 , 10.00492778 , 403 , 12.22909535
404 , 11.56874792 , 405 , 14.87138889 , 406 , 12.80590278 , 407 , 13.30902778

408 , 14.44069444 , 409 , 13.33708333 , 410 , 13.74277778 , 411 , 15.10743056
412 , 15.16805556 , 413 , 14.11868056 , 414 , 14.12944444 , 415 , 14.84166667
416 , 13.79659722 , 417 , 14.58958333 , 418 , 15.29423611 , 419 , 15.44020833
420 , 15.67222222 , 421 , 14.37958333 , 422 , 14.13 , 423 , 15.90395833
424 , 16.15534722 , 425 , 15.07284722 , 426 , 13.81583333 , 427 , 14.356875
428 , 15.24534722 , 429 , 15.79583333 , 430 , 15.26798611 , 431 , 15.54527778
432 , 15.92548611 , 433 , 16.32743056 , 434 , 15.24729167 , 435 , 19.20840278
436 , 17.04208333 , 437 , 14.525 , 438 , 13.89555556 , 439 , 14.62069403
440 , 16.08034722 , 441 , 15.90083333 , 442 , 17.29666667 , 443 , 19.27673611
444 , 20.355625 , 445 , 19.71006944 , 446 , 17.75916667 , 447 , 19.05166667
448 , 19.80659722 , 449 , 20.78583333 , 450 , 21.90895833 , 451 , 21.04993056
452 , 22.25506944 , 453 , 22.55090278 , 454 , 21.84111111 , 455 , 21.47875
456 , 18.65256944 , 457 , 17.94777778 , 458 , 19.23555556 , 459 , 17.37784722
460 , 16.33381944 , 461 , 17.55645833 , 462 , 17.75555556 , 463 , 16.65194444
464 , 16.89215278 , 465 , 12.6066659 , 466 , 12.37969847 , 467 , 14.13881771
468 , 15.08604167 , 469 , 14.12229167 , 470 , 13.20166507 , 471 , 15.08166667
472 , 14.69541667 , 473 , 13.46979167 , 474 , 13.17722222 , 475 , 13.83118056
505 , 12.15180556 , 536 , 5.041427778 , 566 , 5.756739792 , 597 , -2.687569444
628 , -3.773554278, 656 , 1.164978085 , 687 , 5.264088542 , 717 , 11.96541389
748 , 14.18749785 , 778 , 14.11868056 , 809 , 20.355625 , 840 , 13.83118056
870 , 12.15180556 , 901 , 5.041427778 , 931 , 5.756739792 , 962 , -2.687569444
993 , -3.773554278, 1021, 1.164978085 , 1052, 5.264088542 , 1082, 11.96541389
1113, 14.18749785 , 1143, 14.11868056 , 1174, 20.355625 , 1205, 13.83118056
1235, 12.15180556 , 1266, 5.041427778 , 1296, 5.756739792 , 1327, -2.687569444
1358, -3.773554278, 1386, 1.164978085 , 1417, 5.264088542 , 1447, 11.96541389
1478, 14.18749785 , 1508, 14.11868056 , 1539, 20.355625 , 1570, 13.83118056
1600, 12.15180556 , 1631, 5.041427778 , 1661, 5.756739792 , 1692, -2.687569444
1723, -3.773554278, 1751, 1.164978085 , 1782, 5.264088542 , 1812, 11.96541389
1843, 14.18749785 , 1873, 14.11868056 , 1904, 20.355625 , 1935, 13.83118056
1965, 12.15180556 , 1996, 5.041427778 , 2026, 5.756739792 , 2057, -2.687569444
2088, -3.773554278, 2116, 1.164978085 , 2147, 5.264088542 , 2177, 11.96541389
2208, 14.18749785 , 2238, 14.11868056 , 2269, 20.355625 , 2300, 13.83118056
2330, 12.15180556 , 2361, 5.041427778 , 2391, 5.756739792 , 2422, -2.687569444
2453, -3.773554278, 2481, 1.164978085 , 2512, 5.264088542 , 2542, 11.96541389
2573, 14.18749785 , 2603, 14.11868056 , 2634, 20.355625 , 2665, 13.83118056
2695, 12.15180556 , 2726, 5.041427778 , 2756, 5.756739792 , 2787, -2.687569444
2818, -3.773554278, 2846, 1.164978085 , 2877, 5.264088542 , 2907, 11.96541389
2938, 14.18749785 , 2968, 14.11868056 , 2999, 20.355625 , 3030, 13.83118056
3060, 12.15180556 , 3091, 5.041427778 , 3121, 5.756739792 , 3152, -2.687569444
3183, -3.773554278, 3211, 1.164978085 , 3242, 5.264088542 , 3272, 11.96541389
3303, 14.18749785 , 3333, 14.11868056 , 3364, 20.355625 , 3395, 13.83118056
3425, 12.15180556 , 3456, 5.041427778 , 3486, 5.756739792 , 3517, -2.687569444
3548, -3.773554278, 3576, 1.164978085 , 3607, 5.264088542 , 3637, 11.96541389
3668, 14.18749785 , 3698, 14.11868056 , 3729, 20.355625 , 3760, 13.83118056
3790, 12.15180556 , 3821, 5.041427778 , 3851, 5.756739792 , 3882, -2.687569444
3913, -3.773554278, 3941, 1.164978085 , 3972, 5.264088542 , 4002, 11.96541389
4033, 14.18749785 , 4063, 14.11868056 , 4094, 20.355625 , 4125, 13.83118056
**
**

Appendix H. Matlab program: Tendon stresses

```
%%%%%%%%%%%%%%%%%%%%%%%%%%%%%%%%%%%%%%%%%%%%%%%%%%%%%%%%%%%%%%%%%%%%%%%%%%%%%%%%
%%                                                                              %%
%%  MATLAB PROGRAM TO CALCULATE THE SRESSES IN THE TENDONS                      %%
%%  ACCORDING TO Bilfinger Berger (2003).                                       %%
%%                                                                              %%
%%  PROGRAMMED BY:                                                              %%
%%                  CANOVIC SENAD                                               %%
%%                  GONCALVES JOAKIM                                            %%
%%                                       GOTHENBURG,SWEDEN 2004 ©               %%
%%                                                                              %%
%%%%%%%%%%%%%%%%%%%%%%%%%%%%%%%%%%%%%%%%%%%%%%%%%%%%%%%%%%%%%%%%%%%%%%%%%%%%%%%%
clear all
clc

%%INPUT DATA:
%%Number of strands in a tendon
amount=22;
%%Force in a strand in bars
Fbar=100;

%%CALCULATIONS:
%%Total area of a tendon
A=amount*0.140E-3
%%Force in one strand in kN according to Bilfinger Berger (2003)
FkN=(Fbar-4.9849)/2.2153
%%Total force in a tendon
FkNtot=amount*FkN
%%Stress in a tendon
SPa=(FkNtot*1000)/A
```

Appendix I. ABAQUS input file for boundary conditions and definition of spring elements.

```
********************************** BOUNDARY CONDITIONS*****************
**
**   Fixed D.O.F.s for supports at end abutments, pier and arch foundations,
**   and rock anchors
**
** Variable definitions:
** *BOUNDARY
** node no,  first fixed D.O.F.,  last fixed D.O.F.
**
** Arch foundations:
*BOUNDARY
3001,1,4
3001,6
3117,1,4
3117,6
**********************************SPRING ELEMENTS**********************
**
**
*ELEMENT,TYPE=SPRING1,ELSET=S3001-5
73001,3001
*SPRING, ELSET=S3001-5
5
9.60E+11
**
**
*ELEMENT,TYPE=SPRING1,ELSET=S3117-5
73002,3117
*SPRING, ELSET=S3117-5
5
9.60E+11
**
**
```

Appendix J. ABAQUS input file for cross section.

```
***************CROSS SECTIONAL GEOMETRY FOR ARCH****************************
**
**
** DEFINITION OF CROSS SECTIONAL GEOMETRY
** For the arch and piers, the element cross-sectional geometry is
** the mean value from the end sections.
** For other elements, the cross-sectional constants for the first node is
** used.
** Approximate element normal n1, taken as the normal for the first element
** with the current cross-section.
**
** Variables defined on data-lines:
** *BEAM SECTION (Def of cross-sectional geometry, element axes)
** a (width), b (height), t1 (web thickness), t2 (upper flange thickness),
** t3 (web thickness), t4 (lower flange thickness)
** n1x , n1y , n1z
**
**
** ARCH CROSS-SECTIONS
** Cross-sectional properties calculated as mean values of adjacent sections
**
**
*BEAM SECTION, ELSET=A301, MATERIAL=SS0, SECTION=BOX
6.282,       4.232,     1.526,      1.116,      1.526,      1.116
0.000,      -1.000,     0.000



*****CROSS SECTIONAL GEOMETRY AND MATERIAL DATA FOR AUXILIARY CROSS BEAMS*****
**
**
*BEAM GENERAL SECTION,  SECTION=GENERAL,  ELSET=A 530,      DENSITY= 0
 1.0000E+00 ,     8.333E-02  ,      0.000,      8.333E-02,  1.400E-01
-1.000      ,     0.000      ,      0.000
 2.00000E+11,     7.69230E+10,      1.200E-05
*CENTROID
      0.0,  0.0
*SHEAR CENTER
      0.0,  0.0
*TRANSVERSE SHEAR STIFFNESS
      6.41E+10,   0.00E+00



***************CROSS SECTIONAL GEOMETRY FOR TENDONS*************************
**    ELSET=A6xx
**    XX=NUMBER OF STRANDS IN A TENDON
**
**
*SOLID SECTION    ,  MATERIAL=STEEL,  ELSET=A602
      0.2800E-03  ,
```